American Mineralogist, Volume 82, pages 213–244, 1997

REVIEW

Theory of displacive phase transitions in minerals

MARTIN T. DOVE

Department of Earth Sciences, University of Cambridge, Downing Street, Cambridge CB2 3EQ, U.K.

ABSTRACT

A lattice-dynamical treatment of displacive phase transitions leads naturally to the soft-mode model, in which the phase-transition mechanism involves a phonon frequency that falls to zero at the transition temperature. The basic ideas of this approach are reviewed in relation to displacive phase transitions in silicates. A simple free-energy model is used to demonstrate that Landau theory gives a good approximation to the free energy of the transition, provided that the entropy is primarily produced by the phonons rather than any configurational disorder. The ''rigid unit mode'' model provides a physical link between the theory and the chemical bonds in silicates and this allows us to understand the origin of the transition temperature and also validates the application of the soft-mode model. The model is also used to reappraise the nature of the structures of high-temperature phases. Several issues that remain open, such as the origin of first-order phase transitions and the thermodynamics of pressure-induced phase transitions, are discussed.

INTRODUCTION

The study of phase transitions extends back a century to the early work on quartz, ferromagnets, and liquid-gas phase equilibrium. Given the importance of quartz to mineralogy, one can say that the history of the study of phase transitions in minerals is as old as the very subject of phase transitions itself (Dolino 1990). Yet despite this historical link, much of the progress in our *understanding* of phase transitions developed in the fields of solid-state physics and solid-state chemistry has not, until recently, had a great impact in mineralogy and mineral physics, even though the catalog of minerals is riddled with phase transitions. The different types of phase transitions found in minerals are similar in many respects to the phase transitions observed in ionic, metallic, and molecular crystals, and they include displacive phase transitions, cation ordering transitions (for example, Al-Si and Na-K), and orientational order-disorder phase transitions. Several examples of the different types of phase transitions observed in minerals are given in Appendix 1, some of which are illustrated in Figure 1.

This review article is primarily concerned with displacive phase transitions, which involve only small motions of atoms to change the symmetry of a crystal structure. My aim is to present, in a simplified manner, some of the theoretical ideas that underpin the recent applications of solid-state physics to the study of displacive phase transitions in minerals. Examples are the phase transitions observed in quartz, cristobalite, and leucite, which are represented in Figure 1. In each case, the phase transitions involve small translations and rotations of the $(Si,Al)O_4$ tetrahedra. One of the most popular of the new developments in the theory of displacive phase transitions in minerals is the use of Landau theory to describe the thermodynamics of phase transitions (Putnis 1992; Salje 1990a, 1991a, 1991b, 1992a). This theory gives a phenomenological framework to describe the temperature dependence of a range of thermodynamic and physical quantities, and provides a link between different experimental measurements. It also explains the physical background behind Landau theory. In the case of displacive phase transitions, the idea of the soft mode, namely a phonon mode with a frequency that falls to zero at the phase transition, is of some importance, and I will show how this comes about and how it is linked in with Landau theory. Tied in with the use of new theoretical methods are new experimental approaches, including vibrational spectroscopy (Iqbal and Owens 1984; Salje 1992b) and neutron scattering (Axe 1971; Dorner 1982; Skold and Price 1986; Ghose 1988), and I hope that one positive aspect of this article is to promote wider use of these techniques. I also hope that another message of this article is that the flow of ideas between solid-state physics and mineralogy need not be seen as one-way only, we have in the family of silicates a class of materials that can provide new insights into phase-transition phenomena that will surely have more general applications in the fields of solid-state physics and chemistry.

The study of phase transitions is full of technical points

0003–004X/97/0304–0213$05.00

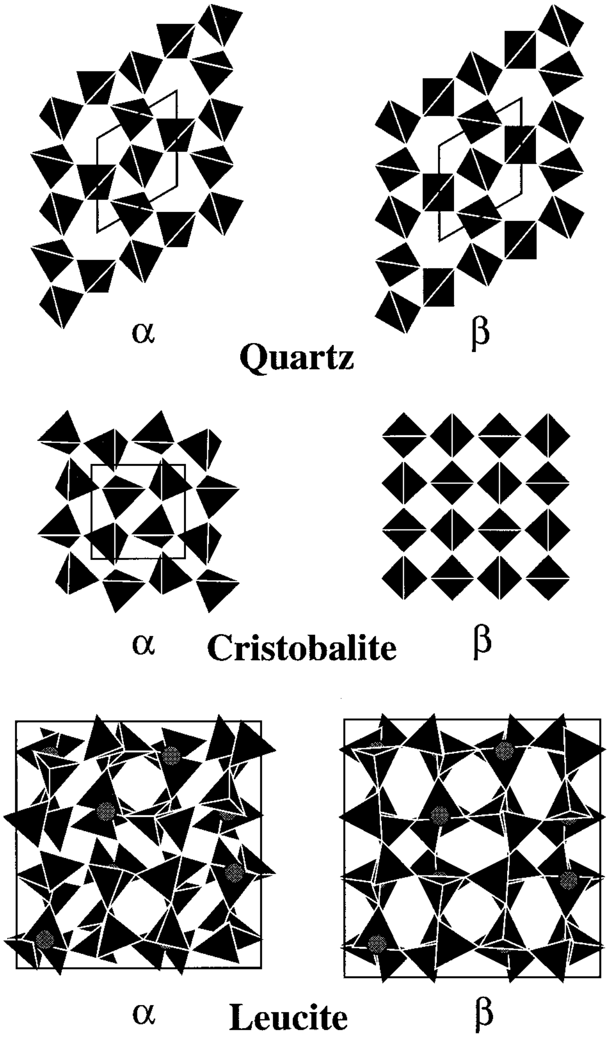

Figure 1. Examples of displacive phase transitions in minerals. In each case α is the low-temperature phase and β is the high-temperature phase. In these examples the displacive phase transitions occur as a result of rotations and translations of the nearly rigid tetrahedra.

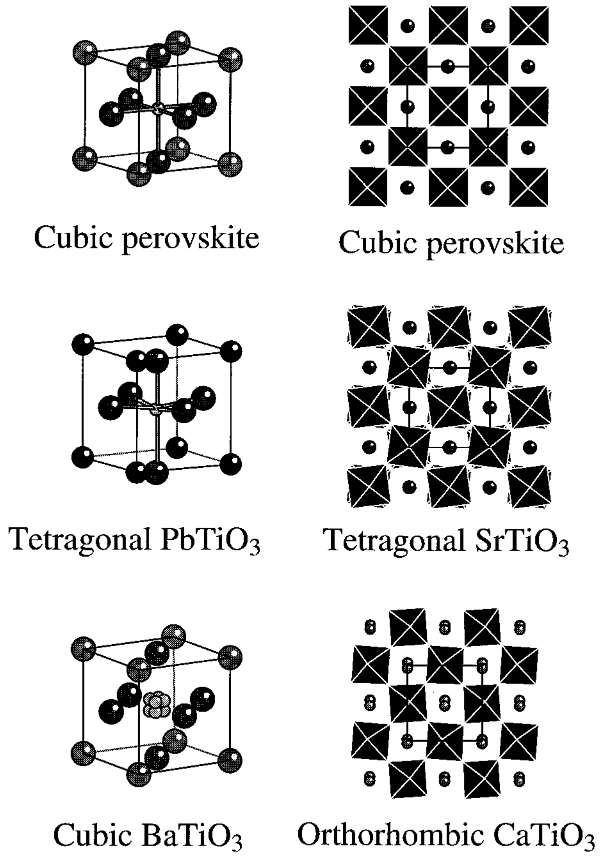

Figure 2. Examples of phase transitions in perovskites, showing the displacive phase transitions involving displacements of cations or rotations of octahedra. The figure for $BaTiO_3$ shows the eight sites for the Ti^{4+} cations in the cubic phase.

that, when not understood or properly defined, lead to ambiguities based on semantics. This problem is illustrated by the displacive phase transitions in the perovskite family (Fig. 2) (Bruce and Cowley 1981; Blinc and Zeks 1974; Lines and Glass 1977). One type of displacive phase transition involves rotations of TiO_6 octahedra about the [001] axis, as in $SrTiO_3$. The actual atomic displacements are small, and it appears that one unit cell behaves in more-or-less the same way as every other. Similar examples are $CaTiO_3$ and $MgSiO_3$, where the octahedra tilt by different amounts about all three axes. Another type of displacive phase transition is seen in $PbTiO_3$ (Shirane et al. 1970; Burns and Scott 1970), in which the Pb^{2+} and Ti^{4+} cations move off-center along [001] to generate a ferroelectric phase transition (a phase transition where the small changes in the atomic positions give rise to the formation of a macroscopic dielectric polarization). $SrTiO_3$ also appears to be trying to undergo the same sort of phase transition at a low temperature (Cowley 1962), but quantum effects, which we discuss later, suppress the transition. These examples are clear enough, but the waters are muddied by the ferroelectric phase transition in $BaTiO_3$ (Yamada et al. 1969; Harada et al. 1971). This example appears at first sight to be very similar to $PbTiO_3$, but in this case it seems that the Ti^{4+} atoms appear to occupy a central site in the high temperature cubic phase only on average, whereas in practice that site is always a potential-energy maximum. The potential-energy minima for the Ti^{4+} cations are located away from the central site along the eight ⟨111⟩ directions, so that in the high-temperature phase the Ti^{4+} cations are hopping among the eight different sites. The ferroelectric phase transition occurs when the Ti^{4+} cations begin to lie preferentially in the sites in the positive *c* direction. There are still four of these, so there are subsequent phase transitions on further cooling until the Ti^{4+} cations all occupy the same one site in the unit cell. Ferroelectric phase transitions that involve the ordering of a proton between the two sites on a double-well hydrogen bond, such as in

KH_2PO_4, are a further extreme example of this (Bruce and Cowley 1981; Blinc and Zeks 1974; Lines and Glass 1977). Some people like to think of all these transitions as displacive, because they all involve small atomic displacements, whereas others consider the one case to be truly displacive and the other to be order-disorder. In this review, I use this latter choice of terms, at least for the extreme cases. The distinction is not based on the actual atomic displacements but on thermodynamic criteria. In the displacive case very little of the entropy will be configurational, whereas in the order-disorder case the entropy is mostly configurational in origin. In practice there may not always be a sharp distinction between the two cases; this is seen by considering a simple model below.

The open questions

The first stage in the investigation of a phase transition is to characterize it experimentally, to determine the transition temperature, to measure directly or indirectly the changes in the structure on cooling below the transition temperature, and perhaps to obtain some thermodynamic data. With a reasonable set of data it may be possible to draw a range of data together within the framework of Landau theory, as described below. Landau theory has proven to be an extremely powerful tool, for with a handful of empirical parameters it may be possible to describe a full set of diverse experimental data for physical and thermodynamic properties over a wide range of temperatures (Putnis 1992; Salje 1990a, 1991a, 1991b, 1992a). The framework of Landau theory may also allow the relationship between different phase transitions in the same material to be understood, such as when there is an Al-Si ordering phase transition and a displacive phase transition.

The second stage in the investigation of a phase transition is to go beyond trying to understand *what* is happening to then try to understand *why* the phase transition occurs, together with a host of other questions that are summarized below. The power of Landau theory is that some questions can be answered by symmetry arguments. For example, the ***c*** axis in calcite (Dove and Powell 1989) expands on heating up to the phase-transition temperature in a way that is determined by the relationship between the symmetry of the expansion of the lattice and the symmetry of the ordering process because of the phase transition. How much it expands may be a function of things like the ionic radius and the amplitude of thermal vibrations, which in turn reflect the atomic masses. Well, there are some questions for which the answer may be ‘‘it just is so’’, but equally there are other questions whose answers lead into deeper physical insights. These are the subject of this review.

Why can phase transitions occur?

It is intriguing to ask why phase transitions should be so common in minerals. If we take the case of framework aluminosilicate minerals, the Si-O and Al-O bonds are strong and the framework structure is reasonably rigid by reason of the connectivity of the strong bonds. In this case the question concerns why there might be easy modes of deformation to allow the phase transition to occur. And even if an easy mode of deformation exists, why would the structure want to distort? Another example is Al-Si ordering phase transitions. Given that the energy required to form Al-O-Al linkages is quite large (of the order of 40 kJ/mol or more; Putnis 1992; Phillips and Kirkpatrick 1995; Dove et al. 1995a), it might be expected that these cations only disorder in equilibrium at temperatures well above the melting points. Yet we find that there is a wide range of ordering temperatures, apparently even to fairly low temperatures. There must be something in these systems that allows for easy disordering and thus allows the phase transition to occur.

What drives the phase transition?

The second question addresses the fact that even if, say, there is an easy mode of deformation to allow a displacive phase transition, there still needs to be some driving force for the phase transition actually to occur. There are two aspects to the driving force. First there must be forces that will locally distort the structure. We saw an example of this in the discussion of the Ti^{4+} cation hopping between sites of local potential energy minima in $BaTiO_3$, where it is the existence of these potential energy minima that give rise to the local distortions of the structure at low temperatures. The second part of the driving force is some interaction that gives a coupling between local ordering processes. There can only be an ordering transition in $BaTiO_3$, say, if the Ti^{4+} cations in neighboring unit cells interact with each other and force each other to order in the same way.

This issue of the coupling between ordering atoms is pertinent for many aluminosilicates where there are cations, such as K^+ and Ca^{2+}, in large cavities formed by the framework of linked SiO_4 and AlO_4 tetrahedra. In these cases, phase transitions often involve both displacements of the cations from the centers of the cavities and collapse of the framework. Thus we can ask what is the driving mechanism, whether it is ordering of the cations or collapse of the framework? It is tempting to think that the cations rattling around in their cavities will like to order. However, the key point is not that there is a local driving force to order single cations, but that there must be some mechanism to couple the ordering of neighboring cations.

What determines the transition temperature?

Linked to the first and second questions is the issue of what actually determines the value of the transition temperature. Given that there is an easy way for a phase transition to occur at an observable temperature, and that there is a driving force to make the transition occur at a finite temperature, we can, in principle, tackle the issue of the factors that give the final value of the transition temperature. At a later point in this review, I will derive an equation for the transition temperature of a displacive phase transition, which involves a large summation over all wave vectors in reciprocal space. Although this equation will link the transition temperature to microscopic quantities, which in one sense will meet some of the aims of this review, we will look beyond this equation to see whether there are any fundamental interactions that will be the main factors in determining the transition temperature.

Why does one phase transition occur in preference to another potential phase transition?

Stokes and Hatch (1989) have used group theoretical methods to determine, for each space group, all the phase transitions that can be obtained by an instability with a wave vector at a symmetry point in the Brillouin zone. For the cubic phase of the mineral leucite, with space group *Ia*3*d*, there are 133 possible phase transitions listed (Stokes and Hatch 1988). Yet leucite samples with similar chemical composition, e.g., $RAlSi_2O_6$ with R = K, Rb, or Cs, undergo the same type of displacive phase transition (Palmer et al. 1997). This suggests that there may be some fundamental reason why the other 132 possibilities do not occur.

Why does Landau theory appear to work well for displacive phase transitions?

We have already remarked that Landau theory has been used successfully to describe many displacive phase transitions in minerals. In essence Landau theory is simply a Taylor expansion of the free energy in terms of a parameter that describes the change in the structure as a result of the phase transition (called the order parameter, as defined below), with the symmetry properties of the phase transition properly taken into account. As a result one could argue it probably should work reasonably well, at least close to the transition temperature when the distortions generated by the phase transition are small. However, it is found that Landau theory works well over a wide range of temperatures for displacive phase transitions (Salje 1986, 1987, 1990a, 1991a, 1991b, 1992a), although this is not so for order-disorder phase transitions such as ferromagnetic phase transitions. The question could perhaps then be rephrased as to why the Taylor expansion is valid over a wide range of temperatures. A related issue concerns the conditions under which the Taylor expansion might not be expected to be valid.

Why does the mean-field approximation work close to the transition temperature?

Landau theory is a member of a class of theories that invoke the mean-field approximation (Bruce and Cowley 1981; Bruce and Wallace 1989; Chaikin and Lubensky 1995; Yeomans 1992). This approximation will be explained in more detail below, for the work reviewed here makes heavy use of it. Thermodynamic and physical properties at temperatures close to the transition temperature tend to follow the general form, $|T - T_c|^\lambda$ where T is the temperature, T_c is the transition temperature, and the value of the exponent l depends on the specific physical property or thermodynamic function (Bruce and Cowley 1981; Bruce and Wallace 1989; Chaikin and Lubensky 1995; Yeomans 1992). All mean-field type theories predict the same set of values for the different exponents. For example, the mean-field theory of ferromagnetism predicts that the magnetization will vary as $|T_c - T|^{1/2}$ and the magnetic susceptibility will vary as $|T - T_c|^{-1}$, regardless of the specific details of the magnetic ordering. Landau theory predicts identical behavior. Indeed, we will find that similar relationships with the same exponents arise in the theory of displacive phase transitions, for these values for the exponents are determined by the use of the mean-field approximation rather than by the details of the phase transition. For magnetic phase transitions, though, it is found experimentally that mean-field theories are not at all accurate for temperatures close to the transition temperature (Bruce and Wallace 1989). The failure of mean-field theory is most easily recognized by the fact that the exponents have values that are very different from those predicted by mean-field theory. For example, at temperatures close to the transition temperature the magnetization is found to vary as $|T_c - T|^\beta$ with $\beta \approx 0.38$, and the susceptibility as $|T - T_c|^\gamma$ with $\gamma \approx 1.3$. The reason for the breakdown of the mean-field approximation in these cases is well understood and will be examined later in this review. However, it is frequently (although not always) found that any breakdown of the mean-field approximation in displacive phase transitions occurs at temperatures too close to the transition temperature to be experimentally observed. Why mean-field theories should work so well at temperatures close to the transition temperatures for displacive phase transitions is another question I attempt to tackle in this review.

What determines whether a phase transition is first-order or second-order?

Within the framework of Landau theory mechanisms exist to describe a phase transition as first-order (with a discontinuous change in the structure and entropy, and hence a latent heat at the transition temperature) or second-order (where the structure of the low-temperature phase merges continuously with that of the high-temperature phase at the phase transition, with no discontinuous change in the entropy and hence with no latent heat). In some cases symmetry allows for the existence of odd-order terms in the Landau free energy that force the phase transition to be first order. Empirically, for the majority of cases where only even-order terms are allowed, the order of a phase transition can be set by the sign of the fourth-order term in the expansion of the free energy. Sometimes the sign of the fourth-order term can be rationalized as a result of the size of the coupling between the order parameter and strain (see below). However, whether there may be some further fundamental factors that determine whether a phase transition is first order or second order is an issue that has been investigated by

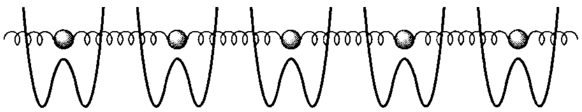

FIGURE 3. Representation of a simple model that undergoes a phase transition in two and three dimensions. The atoms vibrate in double-well potentials (drawn as curves), and interact with their neighbors by harmonic forces, represented as springs. This figure shows the one-dimensional form of the model, but it is easily generalized to higher dimensions.

theory to some extent; I pick up the discussion on this question toward the end of this review.

What is the nature of the high-temperature phase?

My final question concerns the issue of the structural state of a material for temperatures above a displacive phase transition. This is a problem that has aroused considerable controversy from time to time. In some cases it has been suggested that high-temperature phases consist of small domains of the structure of the low-temperature phase in all possible orientations, to give a structure that is averaged over all domains and therefore has the appearance of a higher-symmetry structure. However, the structure of the high-temperature phase could simply be that given by diffraction experiments, or it could be dynamically disordered. Although the question about the nature of the high-temperature phase can only be answered by experiment or by molecular dynamics simulations, I attempt to allow theory to cast some light on this issue.

SIMPLE MODEL AS A PARADIGM FOR PHASE TRANSITION THEORY

A useful tool in the study of the theory of phase transitions is the model illustrated in Figure 3 (Bruce and Cowley 1981; Giddy et al. 1989; Salje 1991b; Padlewski et al. 1992; Radescu et al. 1995). The model contains an array of atoms linked by harmonic forces, with one atom in each unit cell. The model is drawn as a one-dimensional array in Figure 3, but it is easily generalized to two or three dimensions (later it will be shown that the one-dimensional case does not actually have a phase transition). Each atom ‘‘sees’’ a local double-well potential, which is assumed to represent the rest of the crystal that is missing from the model. For example, this double-well potential might represent the potential seen by the Ti^{4+} cation in the perovskite titanates. The double-well potentials provide the driving force for any phase transition. At low temperatures the equilibrium structure has all atoms displaced to one side of their origin or the other. At high temperatures there is a phase transition to a state where each atom vibrates about its origin. Although this model is clearly a gross simplification of what happens in a real crystal, it is actually rather instructive in helping to picture the physical interpretation of the theory and to highlight the issues just raised. I will come back to it several times, and use it as a reference point for comparison. Specifically we will now use this model to clarify the distinction between displacive and order-disorder phase transitions along the lines I mentioned above when comparing the similar perovskites $PbTiO_3$ and $BaTiO_3$, which will be essential in developing a thermodynamic theory of the phase transitions.

The simplest version of this model has a scalar (one-dimensional) displacement of each atom, written as u. The local double-well potential can be represented as

$$V(u) = -\frac{1}{2}\kappa_2 u^2 + \frac{1}{4}\kappa_4 u^4 \qquad (1)$$

where the parameters κ_2 and κ_4 are positive constants. The energy of each atom also includes the harmonic energy because of its interaction with its neighbors, $\tfrac{1}{2}J(u_i - u_j)^2$, where J is the harmonic force constant, and its kinetic energy. The total energy of this system (usually called the Hamiltonian $\mathcal{H}$) is written for the case of a simple cubic arrangement of atoms as

$$\begin{aligned}\mathcal{H} &= \frac{1}{2}\sum_i m\dot{u}_i^2 + \sum_i \left(-\frac{1}{2}\kappa_2 u_i^2 + \frac{1}{4}\kappa_4 u_i^4\right) + \frac{1}{2}\sum_{i\neq j} J(u_i - u_j)^2 \\ &= \frac{1}{2}\sum_i m\dot{u}_i^2 + \sum_i \left(-\frac{1}{2}(\kappa_2 - 6J)u_i^2 + \frac{1}{4}\kappa_4 u_i^4\right) - \sum_{i\neq j} J u_i u_j \end{aligned} \qquad (2)$$

where u_i is the displacement of the ith atom and we consider only the displacement along a single direction. The sum over j is over nearest neighbors only. Each atom has mass m. This model is commonly expressed in both forms given. The first form is similar to most simple lattice dynamics models, whereas the second form is like models for spin systems.

The model defined by Equation 2 has two important quantities (Bruce and Cowley 1981). The first is the depth of the potential well of Equation 1, V_0. The minima of $V(u)$ occur at $u = \pm u_0$, where $u_0^2 = \kappa_2 / \kappa_4$, so that

$$V_0 = -\frac{1}{4}\kappa_2 u_0^2 \qquad (3)$$

The second important quantity is the interaction energy of a pair of atoms with relative displacements u_0 and $-u_0$, which characterizes the strength of the interaction between neighboring atoms:

$$W = 2Ju_0^2 \qquad (4)$$

It is instructive to consider the ratio s of these two quantities:

$$s = \frac{|V_0|}{W} = \frac{\kappa_2}{8J} \qquad (5)$$

This gives the relative strengths of the local double-well potentials and the energy of interaction of an atom with its neighbors (Bruce and Cowley 1981). The factor of ⅛ is not too important, because we will see later that this ratio can be recast as $s \approx |V_0|/k_B T_c$, and we will be thinking about values of s that are large or small compared to unity. Because it may be possible to calculate V_0

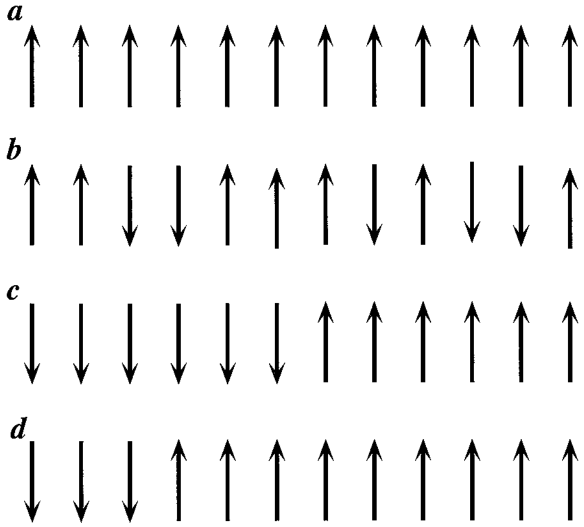

Figure 4. Four different configurations of a chain of spins: (**a**) corresponds to the fully ordered state ($\eta = 1$); (**b**) corresponds to a randomly disordered configuration with $\eta = 0$; (**c**) corresponds to a state with $\eta = 0$ generated from the ordered state by addition of a domain wall in the middle of the chain; (**d**) corresponds to a $\eta = 0.5$ state with generated from the $\eta = 0$ state of configuration *c* by movement of the domain wall.

Figure 5. Sequence showing the ordering of atoms for the model of Figure 3 in the order-disorder limit. At high temperatures ($T \gg T_c$, $\eta = 0$) the positions of neighboring atoms are not correlated in any significant way. On cooling toward the transition temperature ($T > T_c$, $\eta = 0$) the effects of nearest-neighbor interactions become more significant and a degree of short-range order is established. Below the transition temperature ($T < T_c$, $|\eta| > 0$) the probability is greater that one side of the double-well potential (in this case the left-hand side) will be occupied, but there is also a significant probability that some atoms will occupy the alternative potential well. At very low temperatures ($T \ll T_c$) most of the atoms occupy the same side of the double-well potential.

from model interatomic interactions, it may be possible to estimate *s* for any specific example.

Case 1: order-disorder limit

The case $s \gg 1$ corresponds to the order-disorder limit. In this case the potential barrier between the two wells is much higher than the interaction between neighboring atoms. Even at a temperature well above the transition temperature, the atoms will reside in one or other of the two wells, albeit with a random occupancy at first. The examples of $BaTiO_3$ and KH_2PO_4 described earlier are possible examples of this model. Because in this limit the displacements are all $u_i \approx \pm u_0$ for most temperatures, we can represent the simple model by an array of spins, with a spin pointing up for $u_i \approx +u_0$ and pointing down for, $u_i \approx -u_0$, as illustrated in Figure 4. In this case the model Hamiltonian can be represented by the form

$$\mathcal{H} = -\frac{1}{2}\sum_{i,j}\tilde{J}S_iS_j \qquad (6)$$

where $S_i = u_i/u_0 \approx \pm 1$ and $J = 2Ju_0^2$ [it is not necessary now to include the kinetic energy or the single-particle energies because the dominant term is that given in Equation 6]. This is the famous spin-½ Ising model (Yeomans 1992; Chaikin and Lubensky 1995), which is probably the best-studied model of a phase transition. The transition temperature for this model on a cubic lattice has been calculated as

$$k_BT_c(s \gg 1) \approx 4.15Ju_0^2 = 2.255W \qquad (7)$$

Note that k_BT_c is not a direct function of V_0, and indeed $k_BT_c \ll |V_0|$. In the order-disorder limit the effect of the local potential is simply to confine the atoms to one potential well or another. For temperatures in the range, $J \leq k_B\,T \leq V_0$, the particular potential well occupied by a given atom is random with no regard to the potential wells occupied by its neighboring atoms. However, on cooling the effect of the interatomic interaction becomes more important and neighboring atoms begin to prefer to occupy the same side of the double-well potential, giving some degree of short-range order. The spatial range of this short-range order grows on cooling toward T_c, when long-range order is established and the probability of any atom occupying one of the potential wells is larger than the probability of it occupying the other well. This ordering sequence is illustrated in Figure 5.

Case 2: displacive limit

The second case, $s \ll 1$, is the displacive limit. Here the forces between atoms are much larger than the forces due to the local potential. In this case we will later show that the transition temperature in three dimensions is given as

$$k_BT_c(s \ll 1) \approx 1.319Ju_0^2 = 0.6595W \qquad (8)$$

Again the actual height of the potential barrier has nothing to do with the phase transition temperature per se. Unlike in the order-disorder limit, at high temperatures the local potential does not force atoms to sit on one side of the origin or the other, because $|V_0| \ll k_BT_c$. Instead the atoms vibrate about the origin, and the shape of the double-well potential has little effect other than to modify the phonon frequencies. On cooling toward the phase transition, the effects of the shape of the double-well potential become more important and atoms begin to spend relatively more time on either side of the origin. However, because the forces between neighboring atoms are much stronger, neighboring atoms are displaced from the origins by similar amounts. Below the transition temperature the mean positions of all the atoms are displaced by the same small amount to one side of the origin, and the size of this displacement increases on further cooling. This ordering sequence is illustrated in Figure 6.

The model for the displacive limit has many features that are found in a typical displacive phase transition. For example, it has a soft mode of the form that is described later (Padlewski et al. 1992). The free energy has been calculated and found to follow the standard Landau form (Radescu et al. 1995). The model has been studied for a range of parameters using molecular dynamics simulations, with the value of *s* ranging from the extreme displacive limit toward the order-disorder limit (e.g., Padlewski et al. 1992). These studies have provided information on the nature of the high-temperature phases (e.g., Bruce and Cowley 1981).

In passing note that from Equations 7 and 8 we can approximate the ratio *s* in Equation 5 for either limit to $s \approx |V_0|/k_B T_c$, as noted above.

Finally, it will be important to keep in mind the limitations on the model. For example, there is only a single branch of lattice vibrations (as opposed to 3× the number of atoms in the unit cell), and these vibrations are optic modes. Some phase transitions involve an instability of some of the acoustic modes rather than the optic modes; these transitions are called ferroelastic because they involve the formation of a reversible spontaneous shear strain on cooling below the transition temperature (Salje 1990a, 1990b, 1991a, 1991b). Moreover, the simple model does not include any coupling to strain, whereas many phase transitions cause large changes in the lattice parameters. However, we will find that the model is closer to the truth than might be imagined when considering these limitations.

THERMODYNAMIC CONSIDERATIONS

The insights from thermodynamics are of vital importance in our understanding of phase transitions. Much of what is discussed in this review will focus on the calculation of the free energy of a system. The relative free energies of two different phases represent a fine balance between the enthalpy and entropy of the two phases. In the extreme order-disorder case, described for example by Equation 6, the atoms are all displaced to the positions of the minima of the double-well potentials, so that the enthalpy differences between the ordered and disordered phases come directly from the nearest-neighbor interactions, and the entropy is purely configurational. On the other hand, in the displacive case the enthalpy is a more complicated function of direct and indirect interactions between the ordering atoms and the rest of the crystal, and it contains important contributions from changes in the vibrational energy. The entropy now comes from the vibrational contributions rather than from any configurational terms, and changes in entropy through the phase transition arise from the effect of the phase transition on the vibrational spectra. As noted above, the source of the entropy, whether configurational or vibrational, determines whether we think of a phase transition as primarily order-disorder or displacive type.

FIGURE 6. Sequence showing the ordering of atoms for the model of Figure 3 in the displacive limit. At high temperatures ($T \gg T_c$, $\eta = 0$) the atoms vibrate about the zero position, and the effects of the double-well potential are not significant. On cooling toward the transition temperature ($T > T_c$, $\eta = 0$) the effects of double-well potential become more significant and a degree of short-range order is established, where neighboring groups of atoms are temporarily slightly displaced from the origin. Below the transition temperature ($T < T_c$, $|\eta| > 0$) the atoms vibrate about positions that are shifted away from the origin, and all atoms vibrate about the sample displaced point. At very low temperatures ($T \ll T_c$, $\eta = \eta_0$) all the atoms occupy the same side of the double-well potential.

It is interesting to note that how we interpret a phase transition can depend on whether we think of the issues being concerned with what happens on heating up through the phase transition or cooling down below the transition temperature. For example, when we ask why a phase transition occurs, we could start by thinking about the low-temperature phase and ask why there is a process that can disorder the structure, or else we could start by thinking about the high-temperature phase and ask why there might be some displacive instability that occurs at low temperatures. In many cases I will take the perspective of thinking about what happens on cooling from the high-temperature phase. Thus I might ask why the potential $V(u)$ has a double-well form rather than a single minimum at $u = 0$. But sometimes it will be useful to think from the other perspective. For example, given a double-well form of the potential $V(u)$, we could ask why there should be a phase transition on heating at all. Or put another way, why isn't $T_c \approx \infty$?

SCOPE OF THE PRESENT ARTICLE

The objective of this review is to outline the theory of displacive phase transitions as it presently stands, mostly in terms of temperature rather than pressure (see near the end for some comments on this distinction), and to relate the general theory to specific mineralogical examples. Within the field of solid-state physics the general theory has provided a framework for the development of more detailed theoretical models for specific cases, but rarely was there any attempt to tie in numerical predictions with experimental data. Instead the link between experiment and theory has been limited to verification of the general predictions. Historically, it is important to note, in the field of solid-state physics both experiment and theory quickly moved into investigations of the phenomena that are found at temperatures extremely close to the transition temperature, the so-called critical point phenomena (Bruce and Cowley 1981; Bruce and Wallace 1989; Yeomans 1992; Chaikin and Lubensky 1995), leaving some of the above questions unanswered. The main exception is that the link between the general theory and Landau theory was recognized early on, and the conditions for the application of mean-field theory have been appreciated from work on the standard paradigm. Very little of this earlier work has had any impact in mineralogical studies of phase transitions, which in part has prompted the writing of this review. The one part of the theory of phase transitions that has been widely applied within mineralogy is the use of Landau theory. It is not my intention to dwell on Landau theory per se, but it is important to understand the physical basis of this approach, and so one of my objectives is to obtain the main formalism of Landau theory from the general theory of displacive phase transitions. To work within a common context, I give a brief review of Landau theory in the next section. Because there are many other reviews of Landau theory (Blinc and Zeks 1974; Lines and Glass 1977; Bruce and Cowley 1981; Putnis 1992; Salje 1990a, 1991a, 1991b, 1992a) I will focus more on the issues that provide the link with the theory to be developed rather than on the details of the applications of Landau theory.

The general theory of displacive phase transitions is developed in the third section. This is firmly based in the theory of lattice dynamics. The theory answers some of our questions in general terms, but in some respects the theory only leaves us with a sharper question rather than a final solution, not least because the numerical predictions are not straightforward. We have made some progress on this front in the application of the general models to framework silicates, which is the focus of the fourth section. I believe that the insights that come from this single class of materials will have wider applications. In the fifth section I try to link the theoretical ideas with specific experimental studies. Actually the number of relevant experimental studies is small, which again provides a motivation for this review. To close I will discuss the issues that are still open to further investigation. Throughout the review I will highlight answers to the central questions.

Because of constraints on space I need to assume some familiarity with the theory of lattice dynamics, including anharmonic phonon theory, and the statistical mechanics of phonons. I have discussed these topics in some detail elsewhere at a level comparable to that of the present article (Dove 1993), together with an introduction to neutron scattering, vibrational spectroscopy, the different types of phase transitions, and Landau theory. Because the focus of this article is on the general theoretical ideas, I cannot devote much space to the description of specific examples. Many examples are given in Appendix 1, some of which are reviewed in a single volume by Heaney (1994), Hemley et al. (1994), Palmer (1994), and Dolino and Vallade (1994).

LANDAU THEORY OF PHASE TRANSITIONS: BASIC IDEAS, CRITIQUE, AND QUESTIONS RAISED

The order parameter

The essential idea behind Landau theory, at least as envisaged in its early development, is quite simple (Blinc and Zeks 1974; Lines and Glass 1977; Bruce and Cowley 1981; Putnis 1992; Salje 1990a, 1991a, 1991b, 1992a; Dove 1993, Appendix D). A phase transition can be characterized by a parameter, called the order parameter, which contains all the information about the degree of order or extent of deformation in the low-temperature phase. The spirit of Landau theory is that the free energy can be expressed as a low-order Taylor expansion in terms of the order parameter, together with terms that couple the order parameter with other physical quantities (such as strain). The expansion is truncated at the lowest order that is theoretically possible. The behavior of the order parameter and coupled quantities can then be obtained from the free energy using standard thermodynamic relations. It is in this sense that Landau theory has proven to be so powerful: With the minimum of effort a wide range of fundamental relationships can be derived, with coefficients that are usually obtained by fitting experimental data. In the present article the order parameter is given the symbol η; in other cases it is given the symbol Q, but we follow the convention of lattice dynamics and use that symbol for the phonon normal mode coordinate.

The simplest example of a practical definition of an order parameter is for a ferromagnetic phase transition. From a macroscopic perspective we can define the order parameter as the sample magnetization, whereas from a microscopic perspective we can construct an identical definition as

$$\eta = \frac{1}{N}\sum_j S_j \tag{9}$$

where S_j is the value of the spin on the j-th site. In the spin-½ Ising representation, $S_j = \pm S$ (i.e., the atomic moment is assumed to point only up or down), whereas in a more general case both S_j and η are vector quantities.

In the case of a displacive phase transition, the specific definition of the order parameter is a little more ambiguous because of the complicating factors of thermal expansion and the spontaneous strains that frequently accompany displacive phase transitions. Actually the order parameter for the model of Equation 2 does not suffer from these problems, and the order parameter can be defined as the mean displacement:

$$\eta = \frac{1}{N}\sum_j u_j \tag{10}$$

A simple definition for a real material can be constructed by comparing the fractional coordinates of the atoms in the low-temperature and high-temperature phases. For example, in cristobalite (Schmahl et al. 1992) one of the Si atoms has fractional coordinates (*x*, *x*, 0) in the low-temperature phase, which tend toward (¼, ¼, 0) on heating to the high-temperature phase. Thus the order parameter could be defined as

$$\eta = \frac{1}{4} - x \tag{11}$$

By using fractional coordinates rather than absolute displacements we may circumvent the problems associated with thermal expansion. On the other hand, when a transition involves rotations of a group of atoms, such as the TiO_6 octahedra in $SrTiO_3$ or $CaTiO_3$, or SiO_4 tetrahedra in quartz and several other silicates, the order parameter could be equally well defined as the angle $\pm\phi$ that the group of atoms has rotated to break the symmetry (the different signs reflect the fact that neighboring polyhedra must rotate in an opposite sense to maintain a common vertex):

$$\eta = \langle \pm\phi \rangle \tag{12}$$

Because the atomic displacements due to a displacive phase transition are small, all definitions of these types are practically equivalent, and the degree of ambiguity is largely irrelevant. However, some of the displacements and rotations actually follow the order parameter to higher order. For example, models of cristobalite based upon the rotations and translations of rigid SiO_4 tetrahedra show that the changes in one of the fractional coordinates vary quadratically with all the other changes (unpublished analysis). Thus in practice it is essential that one does not simply average over all changes in the atomic positions, but rather one selects only those that have a linear relationship with each other. This set can be selected by calculating the changes in structure assuming perfectly rigid SiO_4 tetrahedra.

The Landau free energy

Having defined an appropriate order parameter, we then assume that the free energy of the low-temperature phase can be written as a power series in the order parameter η:

$$G(\eta) = G_0 + \frac{1}{2}A\eta^2 + \frac{1}{4}B\eta^4 + \cdots \tag{13}$$

where the parameters *A* and *B* are constants, and G_0 is the free energy of the system for $\eta = 0$ (Dove 1993, Appendix D). Usually $G(\eta)$ is independent of the sign of η and therefore only contains terms with even powers of η. There are some cases, however, when $G(\eta) \neq G(-\eta)$, and then terms with odd powers of η must be included in Equation 13, but we will not consider these here (Dove 1993, Appendix D). Equation 13 represents an expansion of the free energy about a maximum value in the low-temperature phase and is therefore expected to be valid only for small values of η, i.e., only close to the phase transition. The free energy of Equation 13 is shown in Figure 7 for two cases, one where $A > 0$, leading to a single minimum at $\eta = 0$, and a second where $A < 0$, leading to a maximum at $\eta = 0$ and minima at non-zero values of η.

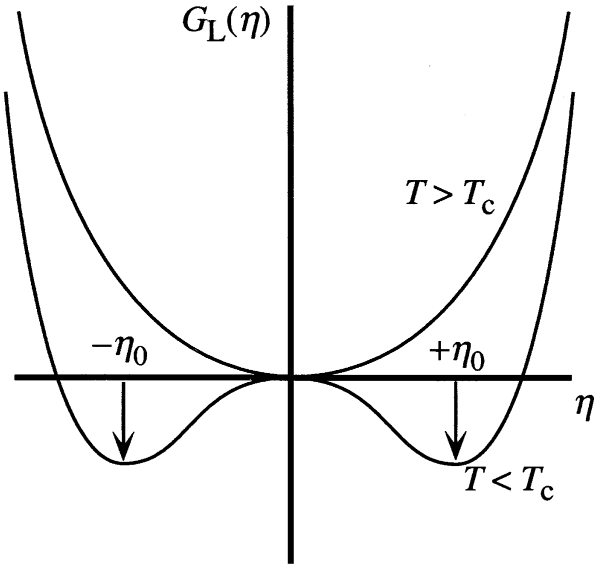

FIGURE 7. Plot of Landau free energy for temperatures above and below the transition temperature. The equilibrium value of the order parameter η is given by the minimum of the free energy. At high temperatures ($T > T_c$) there is a single minimum at $\eta = 0$. At low temperatures ($T \ll T_c$) the free energy has a maximum at $\eta = 0$ and minima at non-zero values of $\eta = \pm\eta_0$.

For the free energy of Equation 13 to represent a phase transition, it is necessary that the value of *A* change sign at the transition temperature, so that it is positive for temperatures above the transition temperature T_c and negative below. The simplest implementation of this condition is to assume that $A = a(T - T_c)$. It is also assumed that we only need to consider the smallest number of terms in the expansion, so that we can rewrite Equation 13 as

$$G(\eta) = G_0 + \frac{1}{2}a(T - T_c)\eta^2 + \frac{1}{4}b\eta^4 \tag{14}$$

where *a* and *b* (= *B*) are positive constants. The equilibrium condition $\partial G / \partial\eta = 0$ applied to Equation 14 leads to the predictions that $\eta = 0$ for $T > T_c$, that there is a continuous (second-order) phase transition at $T = T_c$, and that at lower temperatures η is non-zero and has the temperature dependence:

$$\eta = \left[\frac{a(T_c - T)}{b}\right]^{1/2} \tag{15}$$

When the constant b is negative the form of the free energy gives a discontinuous (first-order) phase transition, and the expansion of the free energy must be taken to higher order (Dove 1993, Appendix D).

Equation 14 can be extended to include more complicated details of symmetry or to account for different vector components of the order parameter. One common extension, keeping within the spirit of expressing the free energy as a simple series expansion and retaining only the lowest-order terms necessary, is to include one or more strain variables, ϵ:

$$G(\eta) = G_0 + \frac{1}{2}a(T - T_c)\eta^2 + \frac{1}{4}b\eta^4 + \frac{1}{2}\zeta\epsilon\eta^n + \frac{1}{2}C\epsilon^2 \tag{16}$$

where ζ and C are constants (C is a normal elastic constant), and n equals 1 or 2 depending on whether the strain has the same or different symmetry to the order parameter. The strain is not an independent quantity when we consider the equilibrium state:

$$\frac{\partial G}{\partial \epsilon} = 0 \Rightarrow \epsilon = \frac{1}{2}\frac{\zeta\eta^n}{C}$$

$$\Rightarrow G(\eta) = G_0 + \frac{1}{2}a(T - T_c)\eta^2 + \frac{1}{4}b\eta^4 - \frac{1}{4}\frac{\zeta^2\eta^{2n}}{C} \tag{17}$$

Hence depending on the value of n, the coupling to strain will either effectively increase the value of T_c ($n = 1$) or reduce the value of the quartic coefficient ($n = 2$). If the effect on the quartic term is so large as to make it negative overall, the phase transition will become first order.

It is common to separate the part of the free energy that contains all the information about η; this is called the Landau free energy G_L:

$$G_L(\eta) = G(\eta) - G_0 \tag{18}$$

The function G_L can be obtained as an approximation to any theoretical free energy. In this review we will derive G_L for a displacive phase transition in terms of microscopic parameters and thereby provide a link between the macroscopic thermodynamic approach and the interatomic forces.

CRITIQUE OF LANDAU THEORY

Landau theory has been widely applied in the solid-state sciences for two main (but not wholly independent) reasons. The first is that for many cases it provides a good empirical description of the observed behavior (Salje 1986, 1987, 1990a, 1991a, 1991b, 1992a). From measurements of the temperature dependence of the order parameter together with thermodynamic data it is quite easy to obtain estimates for the coefficients of the Landau free energy. This approach can lead to a useful rationalization of a number of separate observations. The second reason is that the Landau free energy provides a model free energy that can be developed into a detailed theory. Even when the numerical predictions are not accurate, many of its qualitative predictions are surprisingly useful, because they are based on rigorous principles of symmetry. The use of group theory can give powerful constraints on the formulation of the Landau free energy, leading to some useful predictions concerning many physical properties. At its heart, Landau theory is useful precisely because the free energy is expressed as a Taylor expansion; the central issue then revolves around the extent to which the Taylor expansion can be considered to be valid.

The prediction of the temperature dependence of η, Equation 15, with the exponent of ½, is typical of the predictions of mean-field theories (Bruce and Cowley 1981; Bruce and Wallace 1989; Yeomans 1992; Chaikin and Lubensky 1995), which assume that the individual atoms or magnetic spins that order at the phase transition interact with the average state of all the others. Thus G_L does not contain information about any individual atom, but only about η, which gives an average over all atoms.

We can illustrate this point by considering a simple one-dimensional array of spins, as shown in Figure 4. The order parameter for this example is given by Equation 9. The state $\eta = 1$ (fully ordered) at $T = 0$ K is shown in Figure 4a. Two states with $\eta = 0$ are shown in Figures 4b and 4c. If the spin interactions can be represented by the model Hamiltonian given by Equation 6 with nearest neighbor interactions only, clearly the two configurations with $\eta = 0$ do not have equivalent energy. In Figure 4d we show another state with $\eta = ½$. This state has exactly the same energy as that for $\eta = 0$ shown in Figure 4c. There is, therefore, a range of states with $\eta \neq \pm 1$ that have an equivalent energy. In fact this model has an ordered state only at $T = 0$ K: there is no phase transition at a non-zero temperature.

We can quantify this point by considering the thermodynamic properties of a chain of N spins. If there are n domain walls, each of energy J relative to the energy with complete order, the enthalpy is simply given as nJ and the entropy can be formed by the standard configurational entropy associated with distributing n domain walls on N possible bonds. Minimization of the resultant free energy in the limit $n \ll N$ gives

$$n = N\exp(-J/k_BT) \tag{19}$$

Thus the equilibrium number of domain walls tends to zero only as the temperature goes to zero. The existence of just one domain wall is sufficient to destroy long-range order completely, so long-range order can only occur at $T = 0$ K. Furthermore, it has been shown that no one-dimensional system can undergo a phase transition at a non-zero temperature, and there are a number of model systems that cannot order even in two dimensions (Bruce and Wallace 1989; Thouless 1989; Yeomans 1992; Chaikin and Lubensky 1995). Thus Landau theory fails spectacularly in such cases, since it does not contain any information about dimensionality. One might think that dimensionality is not an issue in mineralogy, but that is not necessarily the case. If ordering forces are sufficiently anisotropic, for example in a chain or layer silicate, the ordering process might be effectively one dimensional at higher temperatures. This is realized for Al-Si ordering in sillimanite, gehlenite, and cordierite (Thayaparam et al. 1994, 1996; Dove et al. 1996a). In these cases, Al-Si ordering is strongest for tetrahedral sites in chains along specific directions. Complete three-dimensional ordering is only made possible by weaker interactions between the chains of tetrahedra.

It might be argued that the failure of the Landau free energy outlined above is partly because G_L is only supposed to work for temperatures close to T_c. However, it is sometimes found experimentally that the temperature dependence of η given by Equation 15 holds for a range of temperatures below T_c, but at temperatures very close to T_c it is no longer described by Equation 15, but by the general form:

$$\eta = A(T_c - T)^{\beta} \tag{20}$$

with $\beta < ½$, typically of the order (but not exactly equal to) ⅓ for three-dimensional systems. The range of temperatures over which the order parameter is described by Equation 20, rather than by Equation 15, is called the Ginzburg interval or critical region (Bruce and Cowley 1981). The existence of the Ginzburg interval is due to spatial fluctuations of the order parameter similar to those shown in Figure 4. The Ginzburg interval is large in spin systems and systems with short-range interactions, but it is found that there are many phase transitions, including phase transitions in minerals, where the Ginzburg interval is so close to zero in size that it cannot be observed.

Even when Landau theory appears to be in reasonable agreement with experiment for most temperatures, Equation 15 cannot work at low temperatures because the third law of thermodynamics requires that $\partial\eta/\partial T = 0$ at $T = 0$ K. Thus G_L is not a correct thermodynamic function, but is an approximation to one at high temperatures. For G_L to be a correct thermodynamic function it must obey the condition that $\partial G_L/\partial T = -\partial G_0/\partial T$ at $T = 0$ K so that $\partial G/\partial T = 0$. For this to be true, then the function G_0 must contain information about η, which contradicts our initial assumption, or else both differentials should tend to zero at $T = 0$ K, which is not the case in the standard Landau formalism.

Despite the fact that I have raised several criticisms of Landau theory, it is often found that displacive phase transitions in many minerals can be described reasonably well by Landau theory. Indeed, it is often found that the order parameter can be described by Equation 15 for temperatures down to 100–200 K, when the effects of the third law of thermodynamics become important.

LATTICE DYNAMICAL THEORY OF DISPLACIVE PHASE TRANSITIONS

Soft-mode theory of displacive phase transitions

Since the classic papers by Cochran (1959, 1960, 1981) on the origin of ferroelectricity, displacive phase transitions have been understood in terms of the soft-mode theory (Blinc and Zeks 1974; Scott 1974; Lines and Glass 1977; Bruce and Cowley 1981; Ghose 1985; Dove 1993, Chapter 8). Historically the theory was partly driven by developments in the understanding of lattice dynamics that followed from the development of inelastic neutron scattering techniques (Axe 1971; Shirane 1974; Dorner 1982; Skold and Price 1986; Ghose 1988). The central idea is that in the high-temperature phase there is a lattice vibration for which the frequency falls to zero on cooling toward the transition temperature. A vanishing frequency implies a vanishing restoring force against the corresponding deformation, which is the reason that vibration is called a soft mode. The atomic displacements associated with the soft mode are the same as the deformation of the structure in the low-temperature phase. For example, in the high-temperature phase of $PbTiO_3$ the soft mode involves the Pb^{2+} and Ti^{4+} cations moving along [001] with the O anions moving in the opposite direction. This is the distortion that freezes into the structure in the low-temperature phase. There is a soft mode in the low temperature phase, which corresponds to the same atomic motions but now vibrating about new mean positions. In the case of $PbTiO_3$ the soft mode in the high-temperature phase is degenerate, so two corresponding modes are observed in the low-temperature phase. The soft modes in both phases have been measured by inelastic neutron scattering (Shirane et al. 1970) and Raman scattering (Burns and Scott 1970; see Fig. 8.8 in Dove 1993).

Anharmonic phonon theory and the soft mode

The energy associated with the lattice vibrations of a crystal is usually expressed in terms of the Hamiltonian for phonons, $\mathcal{H}_{\mathrm{ph}}$, which is written as an expansion of the crystal energy in normal mode coordinates. We first must define terminology. For a crystal containing N unit cells, there are N values of the wave vector $\mathbf{k}$. If the same crystal has Z atoms in the unit cell, there are $3Z$ phonon branches. Each phonon branch is then labelled by ν. Thus each phonon mode is labelled by the wave vector and branch as $(\mathbf{k}, \nu)$. To make the equations compact, we denote $(\mathbf{k}, \nu)$ by k, and $(-\mathbf{k}, \nu)$ by $-k$. The amplitude of each phonon k is represented by the mass-weighted normal-mode coordinate (Dove 1993, Chapter 4). The general anharmonic form can be written as (Dove 1993, Chapter 8)

$$\mathcal{H}_{\mathrm{ph}} = \frac{1}{2}\sum_{k} \omega_k^2 Q_k Q_{-k} + \sum_{s\geq 3}\frac{1}{s!}\sum_{k_1}\cdots\sum_{k_s} V_s(k_1, \cdots, k_s) \cdot Q_{k_1}\cdots Q_{k_s}\Delta(\mathbf{k}_1 + \cdots + \mathbf{k}_s). \tag{21}$$

The first term is the normal harmonic energy, where ω_k

is the harmonic frequency for the phonon k. The remaining terms are the anharmonic components of the energy, each of order s, where V_s is an energy prefactor, and $\Delta(\mathbf{G})$ is a function of value unity if $\mathbf{G}$ is a reciprocal lattice vector and zero otherwise. Technically $\mathcal{H}_{\mathrm{ph}}$ should also contain the kinetic energy term $\frac{1}{2}\Sigma_k \dot{Q}_k \dot{Q}_{-k}$, but because we will not make use of this term we will not include it in our equations. In principle the sum over s in Equation 21 extends to infinite order, but in practice it is usual to include only the terms for $s = 3$ and $s = 4$. For the soft-mode theory the dominant terms are those with $s = 4$, which are the only ones we will consider, so we write

$$\mathcal{H}_{\mathrm{ph}} = \frac{1}{2}\sum_k \omega_k^2 Q_k Q_{-k} + \frac{1}{4!}\sum_{\substack{k_1,k_2\\ k_3,k_4}} V_4(k_1, k_2, k_3, k_4) \cdot Q_{k_1} Q_{k_2} Q_{k_3} Q_{k_4} \Delta(\mathbf{k}_1 + \mathbf{k}_2 + \mathbf{k}_3 + \mathbf{k}_4) \qquad (22)$$

To make progress pairs of normal mode coordinates in the fourth-order term in Equation 22 are replaced by their thermal averages, to give an effective Hamiltonian (Blinc and Zeks 1974):

$$\mathcal{H}_{\mathrm{ph}}^{\mathrm{eff}} = \frac{1}{2}\sum_k \omega_k^2 Q_k Q_{-k} + \frac{1}{4}\sum_k \sum_{k'} \cdot V_4(k, -k, k', -k')\langle Q_{k'} Q_{-k'}\rangle Q_k Q_{-k}. \qquad (23)$$

The coefficient $\frac{1}{4!}$ in Equation 22 has been replaced by $\frac{1}{4}$ to account for the number of possible permutations of the averaging (Blinc and Zeks 1974). Conservation of crystal momentum requires that $\langle Q_k Q_{k'}\rangle$ is only non-zero if $k' = -k$, and that the only terms allowed in the harmonic Hamiltonian are those of the form $Q_k Q_{-k}$. The thermal average is given in phonon theory by the relation

$$\langle Q_{k'} Q_{-k'}\rangle = \frac{\hbar}{\tilde{\omega}_{k'}}\left[n(\tilde{\omega}_{k'}, T) + \frac{1}{2}\right] \approx \frac{k_{\mathrm{B}}T}{\tilde{\omega}_{k'}^2} \quad \text{when } k_{\mathrm{B}}T \geq \hbar\tilde{\omega}_{k'} \qquad (24)$$

where $\tilde{\omega}_k$ is the frequency taking account of the anharmonic interactions, and $n(\omega, \mathrm{T})$ is the Bose-Einstein factor (Dove 1993, Chapter 4). Thus in the high-temperature limit Equation 23 can be written as

$$\mathcal{H}_{\mathrm{ph}}^{\mathrm{eff}} = \frac{1}{2}\sum_k \omega_k^2 Q_k Q_{-k} + \frac{k_{\mathrm{B}}T}{4}\sum_k \sum_{k'} V_4(k, -k, k', -k') Q_k Q_{-k}/\tilde{\omega}_{k'}^2 \qquad (25)$$

This is actually in the same form as a harmonic Hamiltonian and can therefore be rearranged to give

$$\mathcal{H}_{\mathrm{ph}}^{\mathrm{eff}} = \frac{1}{2}\sum_k \left[\omega_k^2 + \frac{k_{\mathrm{B}}T}{2}\sum_{k'} V_4(k, -k, k', -k')/\tilde{\omega}_{k'}^2\right] Q_k Q_{-k} = \frac{1}{2}\sum_k \tilde{\omega}_k^2 Q_k Q_{-k}. \qquad (26)$$

This relation now defines the set of frequencies $\tilde{\omega}_k^2$ used above, these are called the renormalized phonon frequencies, and the model as sketched is called renormalized phonon theory (alternative names are quasiharmonic phonon theory or pseudoharmonic phonon theory). The renormalized frequencies now have an explicit temperature dependence directly extracted from Equation 26:

$$\tilde{\omega}_k^2 = \omega_k^2 + \frac{k_{\mathrm{B}}T}{2}\sum_{k'} V_4(k, -k, k', -k')/\tilde{\omega}_{k'}^2 \qquad (27)$$

This equation has a self-consistent set of solutions for the renormalized frequencies, although in practice it is common to replace the renormalized frequencies in the denominator by their harmonic values (Blinc and Zeks 1974).

It should be appreciated that the temperature dependence I have introduced is quite different from that due to thermal expansion, although thermal expansion is, of course, also an anharmonic effect. In general the increase of the crystal volume on heating leads to a reduction of the phonon frequencies, whereas the direct anharmonic interactions considered here lead to an increase in phonon frequencies on heating. In most cases the indirect anharmonic effects mediated through the thermal expansion dominate, but for phase transition theory it is the direct interactions that are important. These interactions are not included in modeling techniques that assume that the full anharmonicity can be accounted for in the thermal expansion (such as in free-energy minimization techniques).

We now consider the behavior of the soft modes. A crystal structure that is unstable against a small displacive distortion will have a corresponding imaginary harmonic frequency (Dove 1993, Chapter 8). This is seen from the harmonic term in Equation 21. If the crystal is unstable against a small displacive distortion that can be expressed as a normal mode coordinate, the harmonic term $\tilde{\omega}_k^2 Q_k Q_{-k}$ must have a maximum energy when the normal mode coordinate Q_k has a value of zero. This is only possible if $\omega_k^2 < 0$, that is, the phonon frequency $\tilde{\omega}_k$ has an imaginary value. We see from Equation 27 that the anharmonic interactions increase the phonon frequency on heating if $V_4 > 0$. Thus if $\tilde{\omega}_k$ has an imaginary value at $T = 0$ K, the anharmonic interactions will make the frequency become real for temperatures greater than T_{c}, the temperature at which $\tilde{\omega}_k^2 = 0$ in Equation 27:

$$T_{\mathrm{c}} = -2\omega_k^2 \Big/ \left(k_{\mathrm{B}} \sum_{k'} V_4(k, -k, k', -k')/\tilde{\omega}_{k'}^2\right) \qquad (28)$$

At temperatures greater than T_{c} the harmonic mode is stable, $\tilde{\omega}_k^2 > 0$, so the high-symmetry phase is also stable. On the other hand, at low temperatures the crystal is unstable against displacements that are described by the normal mode of label k; we can think about the soft mode being frozen into the structure. Equations 27 and 28 can therefore be rewritten as

$$\tilde{\omega}_k^2 = \left(\frac{k_{\mathrm{B}}}{2}\sum_{k'} V_4(k, -k, k', -k')/\tilde{\omega}_{k'}^2\right)(T - T_{\mathrm{c}}) \qquad (29)$$

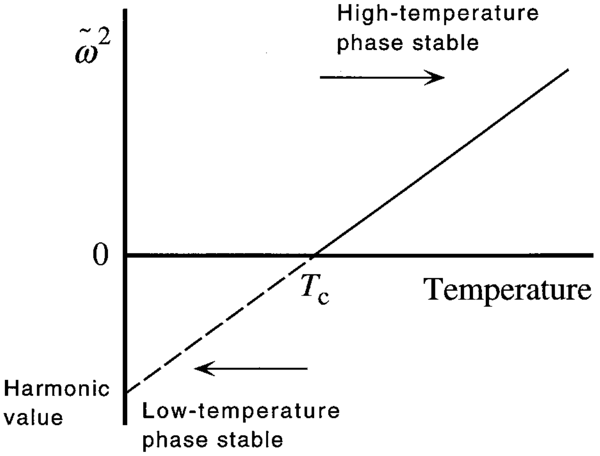

FIGURE 8. Schematic representation of the behavior of the soft mode. At low temperatures ($T \ll T_c$) the soft mode is unstable, which is represented by $\tilde{\omega}$. Thus the structure of the high-temperature phase is unstable. On heating, the anharmonic interactions make a positive contribution to the value of $\tilde{\omega}$, until the frequency reaches zero at the transition temperature (T_c). Above this temperature the soft-mode frequency has a real rather than imaginary value, and the high-temperature phase is stable.

Equation 29 yields the temperature dependence of the soft-mode frequency (Blinc and Zeks 1974; Bruce and Cowley 1981).

The soft-mode model is pictured schematically in Figure 8, where we plot the frequency of the soft mode in the high-symmetry phase as a function of temperature. At $T = 0$ K the structure of the high-symmetry phase is unstable with respect to the distortion to the low-symmetry phase, and the frequency of the soft mode has an imaginary value. On increasing temperature the anharmonic interactions raise the value of $\tilde{\omega}_k^2$. Eventually the contribution of the anharmonic interactions is sufficiently large that the value of $\tilde{\omega}_k^2$ becomes positive, at which point the high-symmetry phase is stable. This defines the transition temperature. Experimentally the soft-mode frequency is found to fall on cooling toward the transition temperature, and it often follows the temperature dependence $\tilde{\omega}_k^2 \propto (T - T_c)$, as predicted by Equation 29.

Experimental data for the soft mode frequency in $SrTiO_3$ are shown in Figure 9 (Fleury et al. 1968; Cowley et al. 1969; Shirane and Yamada 1969). Below the transition temperature the triply-degenerate soft mode splits into two modes, whose frequencies increase with the order parameter ($\omega^2 \propto \eta^2$). The atomic motions associated with the soft mode are the rotations of the TiO_6 octahedra about the three ⟨100⟩ axes.

The standard paradigm

We now draw the connection with the standard paradigm (Bruce and Cowley 1981; Sollich et al. 1994). The normal-mode coordinates are defined as

$$u_{\mathbf{k}} = \frac{\sqrt{m}}{N} \sum_j u_j \exp(i\mathbf{k}\cdot\mathbf{R}_j) \qquad (30)$$

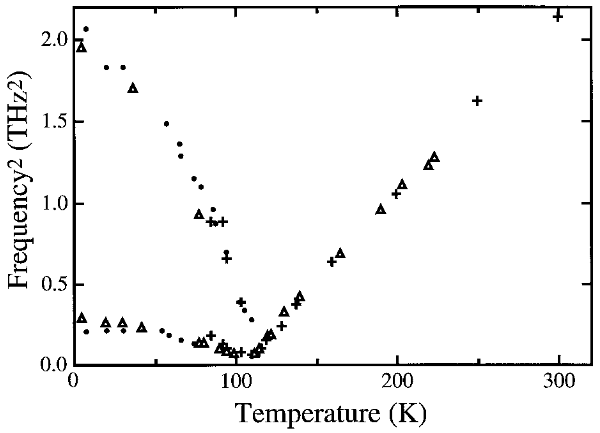

FIGURE 9. Temperature dependence of the soft-mode frequencies in $SrTiO_3$. Data are from Fleury et al. (1968, circles, Raman scattering data), Cowley et al. (1969, crosses, inelastic neutron scattering data), and Shirane and Yamada (1969, triangles, inelastic neutron scattering data).

These give the Fourier transforms of the set of real displacements u_j. The Hamiltonian of Equation 2 [compare with Equation 21] can then be written in the following form, again dropping the kinetic energy term $\frac{1}{2}\Sigma_k \dot{u}_k \dot{u}_{-k}$:

$$\mathcal{H} = \frac{1}{2m} \sum_{\mathbf{k}} (J_{\mathbf{k}} - \kappa_2) u_{\mathbf{k}} u_{-\mathbf{k}} + \frac{\kappa_4}{4m^2} \sum_{\substack{\mathbf{k}_1,\mathbf{k}_2\\ \mathbf{k}_3,\mathbf{k}_4}} u_{\mathbf{k}_1} u_{\mathbf{k}_2} u_{\mathbf{k}_3} u_{\mathbf{k}_4} \Delta(\mathbf{k}_1 + \mathbf{k}_2 + \mathbf{k}_3 + \mathbf{k}_4) \qquad (31)$$

where

$$J_{\mathbf{k}} = \frac{1}{N} \sum_{i,j} J \exp[i\mathbf{k}\cdot(\mathbf{R}_i - \mathbf{R}_j)] \qquad (32)$$

and the sum is restricted to nearest neighbors. The quantity $(J_{\mathbf{k}} - \kappa_2) / m$ is the square of the harmonic frequency of the vibration with wave vector $\mathbf{k}$. In the case where the force constants J are positive, $J_{\mathbf{k}} = 0$ when $\mathbf{k} = 0$, and this is the wave vector of the soft mode. Comparing with Equation 22 for the general case, κ_4 is equivalent to V_4 (k_1, k_2, k_3, k_4) but is independent of the wave vectors.

Following the methods outlined above, the effective Hamiltonian can be written as

$$\begin{aligned} \mathcal{H}^{\mathrm{eff}} &= \frac{1}{2m} \sum_{\mathbf{k}} (J_{\mathbf{k}} - \kappa_2) u_{\mathbf{k}} u_{-\mathbf{k}} + \frac{6\kappa_4}{4m^2} \sum_{\mathbf{k},\mathbf{k}'} \langle u_{\mathbf{k}'} u_{-\mathbf{k}'} \rangle u_{\mathbf{k}} u_{-\mathbf{k}} \\ &\approx \frac{1}{2m} \sum_{\mathbf{k}} \left[(J_{\mathbf{k}} - \kappa_2) + \frac{3\kappa_4 k_B T}{m} \sum_{\mathbf{k}'} J_{\mathbf{k}'}^{-1} \right] u_{\mathbf{k}} u_{-\mathbf{k}}. \end{aligned} \qquad (33)$$

The transition temperature for this model is then given as

$$k_B T_c = \frac{m\kappa_2}{3\kappa_4} / \left(\frac{1}{N} \sum_{\mathbf{k}} J_{\mathbf{k}}^{-1} \right). \qquad (34)$$

For the case of the three-dimensional cubic lattice, the denominator has the value $1.979/J$, and because $\kappa_2 / \kappa_4 = u_0^2$ this gives a derivation of Equation 8. The denominator in fact plays the same role as $\tilde{\omega}^{-2}$ in Equations 27 and

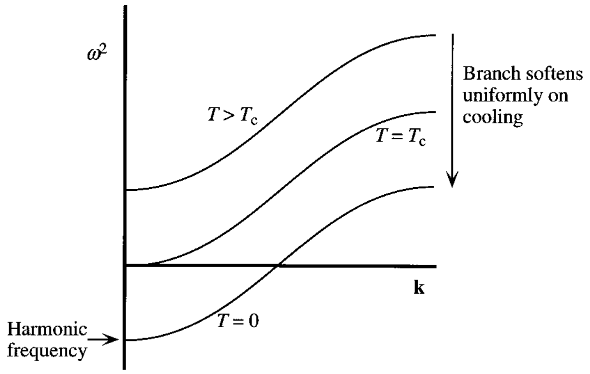

FIGURE 10. Uniform movement of the whole phonon branch with temperature in the standard paradigm.

28. The whole branch changes with temperature uniformly as

$$\tilde{\omega}_{\mathbf{k}}^2 = J_{\mathbf{k}} - \kappa_2 + 3\kappa_4 k_B T \sum_{\mathbf{k}'} \tilde{\omega}_{\mathbf{k}'}^{-2} \qquad (35)$$

This behavior is illustrated in Figure 10 and is the consequence of the anharmonic coefficient being independent of **k**. In order to determine T_c, as the temperature at which $\tilde{\omega}_{\mathbf{k}'}^2 = 0$, the frequencies to use in the denominator in the last term in Equation 35 are $\tilde{\omega}_{\mathbf{k}'}^2 = J_{\mathbf{k}'}$, which are the values at the transition temperature.

It must be stressed that the results for any phase transition can only be compared with this model with great caution. The model has a softening of a phonon only at a single wave vector, as expressed in the form of $J_{\mathbf{k}}$, Equation 32. In practice the phonon surface may be more complicated, for example, in the perovskites there is a soft phonon all across the edges of the Brillouin zone. Any application of this model must be modified to use a suitable functional form for J_k (Sollich et al. 1994).

Lattice dynamics and Landau theory

We now generalize the formalism sketched in this section to consider the low-temperature phase. The dependence of the lattice energy on the order parameter η can again be approximated by the simple double-well potential $V(\eta)$, exactly as in the standard paradigm described earlier:

$$V(\eta) = -\frac{1}{2}\kappa_2\eta^2 + \frac{1}{4}\kappa_4\eta^4. \qquad (36)$$

The coefficient $-\kappa_2$ is now equivalent to the square of the imaginary harmonic frequency. The relevant part of the Hamiltonian can now be written as

$$\mathcal{H} = V(\eta) + \frac{1}{2}\sum_k \omega_k^2 Q_k Q_{-k} + \frac{1}{4}\sum_k \alpha_k Q_k Q_{-k}\eta\eta^* \qquad (37)$$

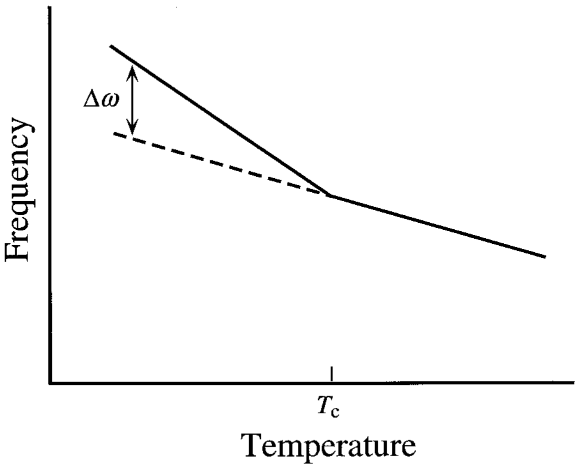

FIGURE 11. Schematic representation of the temperature dependence of a hard-mode frequency.

where we use α_k instead of V_4 to avoid a large parenthetical term. In the high-temperature phase the quantity that becomes the order parameter η in the low-temperature phase plays the same role as any other normal mode coordinate, Q_k. It is not included in the last two terms because the corresponding terms in powers of $Q_k Q_{-k}$ and $|Q_k Q_{-k}|^2$ are explicitly included in $V(\eta)$, with prefactors κ_2 and κ_4 instead of ω_k^2 and α_k, respectively. It is assumed that the phonon frequencies have already been renormalized by their interactions with all the other modes. In the low-temperature phase Equation 37 can be written as

$$\begin{aligned}\mathcal{H} &= V(\eta) + \frac{1}{2}\sum_k\left(\omega_k^2 + \frac{1}{2}\alpha_k\eta\eta^*\right)Q_k Q_{-k} \\ &= V(\eta) + \frac{1}{2}\sum_k \bar{\omega}_k^2 Q_k Q_{-k} \qquad (38)\end{aligned}$$

where

$$\bar{\omega}_k^2 = \omega_k^2 + \frac{1}{2}\alpha_k\eta\eta^*. \qquad (39)$$

The modified frequency $\tilde{\omega}$ carries information about the value of the order parameter (Dove et al. 1992a; Dove 1993, Chapter 8), which provides the basis for the new technique (as applied to mineralogy) of hard-mode spectroscopy (Salje 1992b). From Equation 39 we note that measurements of the way that a phonon frequency at temperatures below the phase transition deviates from the value extrapolated from the frequency in the high-temperature phase gives direct information on the temperature dependence of η, i.e., from equation 39 we can determine the order parameter from $\eta^2 \propto (\tilde{\omega}_k^2 - \omega_k^2) \propto \Delta\omega_k$. This is illustrated in Figure 11. Indeed, measurements of η from changes in phonon frequencies can give the most accurate data on the temperature dependence of η. This is the basis for the use of hard-mode spectroscopy, where the changes in the positions of peaks in Raman and infrared spectra are used to determine the behavior of an order parameter with temperature, annealing time, or chemical composition (Güttler et al. 1989b; Harris et al. 1989, 1990; Palmer et al. 1990; Poon et al. 1990; Redfern and Salje 1992; Redfern 1992; Salje et al. 1992, 1993; Cellai et al. 1995; Zhang et al. 1995).

The virtue of using a quasi-harmonic model is that we can now use the standard expression for the phonon free energy, G_{ph}, of a set of harmonic vibrations:

$$G_{\mathrm{ph}} = \mathrm{k_B}T \sum_k \ln\left[2\sinh\left(\frac{\hbar\omega_k}{2\mathrm{k_B}T}\right)\right]. \tag{40}$$

Note use of the nomenclature of the Gibbs free energy to emphasize the contact with experiment, although technically we are really working with constant volume; the differences are not significant. We now follow the same spirit as Landau theory and expand G_{ph} as a Taylor series in η about the point $\eta = 0$, noting the use of the set of values of $\tilde{\omega}$ as defined by Equation 39 for the frequencies (Dove 1993, Chapter 8). This yields

$$G_{\mathrm{ph}}(\eta) = G_{\mathrm{ph}}(\eta = 0) + \frac{\mathrm{k_B}T}{4}\sum_k \frac{\alpha_k}{\bar{\omega}_k^2}\eta^2 + \cdots \tag{41}$$

To make the nomenclature more transparent, I write Equation 41 in the form of an Einstein model (although I will not actually be making an Einstein approximation):

$$G_{\mathrm{ph}}(\eta) = G_{\mathrm{ph}}(\eta = 0) + \frac{3\mathrm{R}T\tilde{\alpha}}{4\tilde{\omega}^2}\eta^2 + \cdots \tag{42}$$

where

$$\tilde{\alpha} = \frac{1}{3N}\sum_k \alpha_k \tag{43}$$

and

$$\tilde{\omega}^2 = \tilde{\alpha} / \sum_k (\alpha_k/\bar{\omega}_k^2). \tag{44}$$

If we take the part of that depends on η and add this to $V(\eta)$ as defined in Equation (36), we obtain an expression that is equivalent to the Landau free energy:

$$\begin{aligned} G_{\mathrm{L}}(\eta) &= -\frac{1}{2}\kappa_2\eta^2 + \frac{3\tilde{\alpha}\mathrm{R}T}{4\tilde{\omega}^2}\eta^2 + \frac{1}{4}\kappa_4\eta^4 \\ &= \frac{3\tilde{\alpha}\mathrm{R}}{4\tilde{\omega}^2}(T - T_{\mathrm{c}})\eta^2 + \frac{1}{4}\kappa_4\eta^4 \end{aligned} \tag{45}$$

where T_{c} is the transition temperature, given by

$$T_{\mathrm{c}} = \frac{2\kappa_2\tilde{\omega}^2}{3\mathrm{R}\tilde{\alpha}}. \tag{46}$$

This is similar to the form given in Equation 28, where the square of the imaginary soft-mode frequency has now been replaced by $-\kappa_2$.

In principle the expansion of the phonon free energy, Equation 42, can be extended to higher order. This would add a temperature-dependent term to the higher order coefficients in the Landau free energy. The fourth-order coefficient would then be given by

$$b = \kappa_4 - \frac{3\tilde{\alpha}^2\mathrm{R}T}{\tilde{\omega}^4}. \tag{47}$$

The temperature-dependent part of Equation 47 is negligibly small in value compared to the value of κ_4 (see below), so that none of the higher order terms in the expansion of the phonon free energy is important.

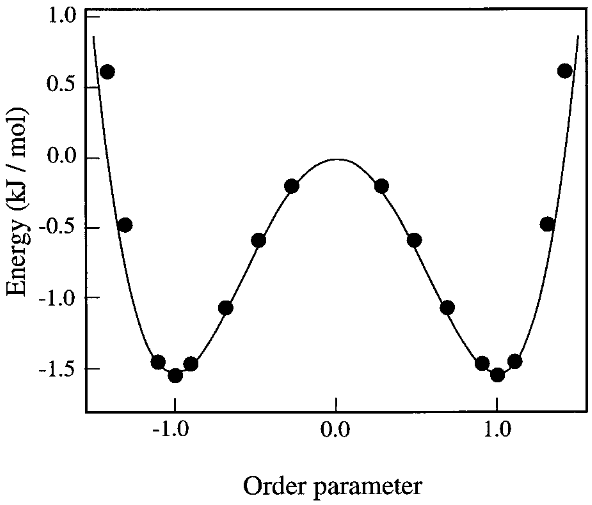

FIGURE 12. The potential energy $V(\eta)$ calculated for quartz using the interatomic potential of Tsuneyuki et al. (1988). The points represent actual calculations, and the curve is a fitted form of Equation (36).

Example calculation for quartz

To illustrate the theory of the previous two sections, I now present a calculation of the Landau free energy function for quartz. Using the interatomic potential of Tsuneyuki et al. (1988) I have calculated the function $V(\eta)$ by performing an energy minimization for various fixed values of the displacement of the O atom from its position in the high-symmetry phase (unpublished calculation). The function is shown in Figure 12, fitted by a curve of the form of Equation (36). The potential energy is represented reasonably well by the polynomial

$$V(\eta) = 1.542 \times \left[-\frac{1}{2}\left(\frac{\eta}{\eta_0}\right)^2 + \frac{1}{4}\left(\frac{\eta}{\eta_0}\right)^4\right]\mathrm{kJ/mol}. \tag{48}$$

The phonon frequencies of the high-symmetry phase were calculated for a set of wave vectors over a fine grid in reciprocal space and also for a small value of η in the low-symmetry phase. Taking the differences between the frequencies gave the result

$$\frac{1}{N}\sum_k (\alpha_k/\omega_k^2) = 0.2922 \tag{49}$$

where N is the total number of modes considered in the calculation (27 000 in this case). It should be noted that the harmonic frequencies were used in this calculation, rather than the renormalized frequencies. Substitution of these values into Equation 46 yields a value for T_{c} of 578 K. This is lower than the experimental value (848 K), but part of this discrepancy is due to the use of the harmonic frequencies in Equation 49. The renormalized frequencies will be larger than the harmonic values. If we trust our calculated value of $\tilde{\alpha}$, the value of $\tilde{\omega}$ required to give the correct transition temperature is larger by only 1 THz, which is a reasonably small value.

We can also comment on the size of the phonon contribution to the fourth-order term in G_L. The calculations for quartz indicate that the fourth-order term is given as

$$b = 6.2 - (1.0 \times 10^{-6}\ \mathrm{K}^{-1})\ T\ \mathrm{kJ/mol}. \quad (50)$$

This demonstrates that for temperatures up to values many times larger than T_c the constant component dominates the whole coefficient.

Quantum effects and saturation of the order parameter at low temperatures

The complete free energy is given by the sum of Equations 36 and 40,

$$G(\eta) = -\frac{1}{2}\kappa_2\eta^2 + \frac{1}{4}\kappa_4\eta^4 + \mathrm{k_B}T\sum_k \ln\left[2\sinh\left(\frac{\hbar\omega_k(\eta)}{2\mathrm{k_B}T}\right)\right]. \quad (51)$$

Although this reduces to the Landau free energy expansion in the high-temperature limit, it also has the correct thermodynamic limiting behavior at low temperatures, where the free energy has the form

$$G(\eta) \approx -\frac{1}{2}\kappa_2\eta^2 + \frac{1}{4}\kappa_4\eta^4 + \frac{1}{2}\sum_k \hbar\bar{\omega}_k(\eta) - \mathrm{k_B}T\sum_k \exp\left[-\frac{\hbar\bar{\omega}_k(\eta)}{\mathrm{k_B}T}\right]. \quad (52)$$

Without the zero-point phonon motion, the equilibrium value of η at $T = 0$ K is simply obtained from the minimum of $V(\eta)$: $\eta = (\kappa_2/\kappa_4)^{1/2}$. Taking account of the zero-point motion means the equilibrium value of η at $T = 0$ K is obtained by minimization of $G(\eta)$, giving

$$\eta^2 = \frac{\kappa_2}{\kappa_4} - \frac{\hbar}{4\kappa_4}\sum_k \frac{\alpha_k}{\bar{\omega}_k}. \quad (53)$$

This is lower than the value obtained from minimization of $V(\eta)$ alone, which gives the first component of the right-hand side of the result. Indeed, the second term in Equation 53 could be large enough relative to κ_2/κ_4 to drive the transition temperature down to 0 K, or suppress the transition entirely. Nevertheless, a soft mode will be observed, but it will never reach zero frequency. At high temperatures it appears to be falling toward zero at a finite temperature, but then as this temperature is approached the frequency will level off. This situation is observed for a ferroelectric soft mode in $SrTiO_3$ (Cowley 1962).

Minimization of Equation 52 yields the low-temperature behavior of η:

$$\eta^2 = \frac{\kappa_2}{\kappa_4} - \frac{\hbar}{4\kappa_4}\sum_k \frac{\alpha_k}{\bar{\omega}_k}\left[1 + 2\exp\left(-\frac{\hbar\bar{\omega}_k}{\mathrm{k_B}T}\right)\right]$$
$$= \eta^2(T = 0) - \frac{\hbar}{2\kappa_4}\sum_k \frac{\alpha_k}{\bar{\omega}_k}\exp\left(-\frac{\hbar\bar{\omega}_k}{\mathrm{k_B}T}\right). \quad (54)$$

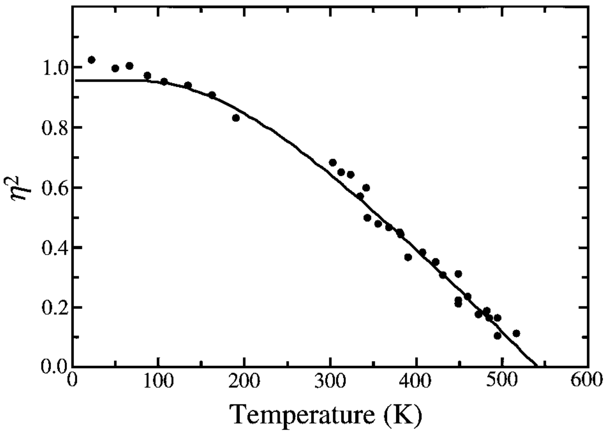

FIGURE 13. Experimental data for the temperature dependence of the square of the order parameter (η^2) in anorthite. The curve is obtained by minimization of the free energy, with adjusted average values of ω and α. The data are from Redfern and Salje (1987).

This has the correct thermodynamic limiting behavior: $\partial\eta/\partial T = 0$ at $T = 0$ K.

Figure 13 shows the application of this model to data for the order parameter in anorthite (Redfern and Salje 1987) over the range of temperatures from nearly 0 K to the transition temperature. An Einstein approximation was used to replace all values of $\bar{\omega}_k$ and α_k by average values ω_{ave} and α_{ave} respectively, which were optimized by comparing values of η obtained from the minimization of $G(\eta)$ to the experimental data. The same problem has been tackled from the perspective of the standard paradigm by Salje and coworkers (Salje et al. 1991; Salje and Wruck 1991; Salje 1991b).

Essential features for the Landau description

The theory developed above is appropriate when all the entropy is phonon entropy, with no contribution from configurational entropy. This is most easily seen in the context of the standard paradigm. In the limit where the stiffness of the forces between atoms is large compared to the local ordering potential, i.e., $s \ll 1$, the phonon theory is the appropriate model to use. In this limit, as we have seen, the Landau polynomial arises as an expansion of the exact free energy. On the other hand, if some degree of configurational entropy is significant because there is some order-disorder component of the phase transition, we will have terms in the free energy of the form

$$G_{\mathrm{config}} = -\mathrm{R}T[(1+\eta)\ln(1+\eta) + (1-\eta)\ln(1-\eta)]$$
$$\approx -\mathrm{R}T[\eta^2 + \eta^4/6]. \quad (55)$$

The configurational terms add a term that varies as $T\eta^2$, similar to that given by the phonon theory, which acts to modify the transition temperature from the value given by Equation 46. However, the configuration terms also add in terms of the form $T\eta^4$ (and of all higher even powers). This means that all the higher-order terms in the

Landau free-energy expansion are temperature dependent. Experimentally, though, it is commonly found that $\eta \propto (T_c - T)^{1/2}$ over a wide range of temperatures. The coefficient of proportionality is given by the ratio of the prefactors on the terms in η^2 and η^4 in the Landau free energy. That this coefficient is found to be largely independent of temperature implies that the prefactors in the Landau free-energy expansion are also independent of temperature, consistent with the view that the entropy associated with displacive phase transitions is mostly vibrational rather than configurational.

Summary of resolved and open issues

The anharmonic phonon theory has led to a picture of the phase transition arising as a result of the anharmonic interactions acting to stabilize a phonon mode that would otherwise be unstable in a purely harmonic model of the high-temperature phase. The phase transition occurs at the temperature at which the soft-mode frequency falls to zero on cooling. Below this temperature the restoring force against the phonon distortion vanishes, and the structure can spontaneously deform. The atomic displacements involved are the same as those associated with the soft phonon.

From the perspectives of the phonon Hamiltonian and the phonon free energy, we have shown how Landau theory follows from the phonon theory of the displacive phase transition, and we have shown how the fundamental parameters in the Landau free energy function are related to the microscopic parameters of phonon theory. The Landau expansion of the free energy with constant coefficients only arises if the entropy is purely vibrational, since the effects of configurational entropy are to make the coefficients in the Landau free energy expansion temperature dependent. The condition for the entropy to be mostly vibrational is that the local double-well potentials should be shallow compared to the strength of the relevant interactions between atoms. We are therefore able to conclude that for displacive phase transitions Landau theory is not simply a phenomenological description but is firmly rooted in the soft-mode theory, and although the parameters of Landau theory may be obtained empirically, they can in principle be related to fundamental quantities. Finally, we have obtained the behavior at low temperatures when quantum mechanics and the third law of thermodynamics become significant and when Landau theory is known to be inappropriate.

We should now think about the things that the theory has not told us. To start with, the phonon theory of displacive phase transitions is a rather nebulous theory. For example, the equation for the transition temperature, Equation 28 or equivalently Equation 46, involves a summation or average of terms for all wave vectors over the whole of reciprocal space. With so many terms involved, it is not easy to relate the final value of the transition temperature to anything fundamental. Indeed, the theory has only been worked out in detail for one case study, $SrTiO_3$ (Bruce and Cowley 1973, 1981). We have not yet discussed the issue of the origin of the double-well potential that is required for a phase transition to occur, nor why this double-well potential is weak compared to the relevant interactions between atoms.

The development of the theory in this section has made no reference to whether the soft mode is an optic mode or an acoustic mode. The idea of the soft mode is usually taken to imply an optic mode, because the soft-mode model was initially conceived within the context of ferroelectric phase transitions (Cochran 1959, 1960, 1981), where the ferroelectric soft mode is actually implied by the Lyddane-Sachs-Teller relation (Lyddane et al. 1941; Dove 1993, Chapter 3). However, for a ferroelastic phase transition the soft mode will be an acoustic mode at $\mathbf{k} = 0$, where the slope of the acoustic mode (and hence the corresponding sound velocity or elastic constant) falls to zero at the transition temperature. The theory must be slightly modified when we have a soft acoustic mode. For example, the coupling constants involving the soft acoustic mode, $V_4(k, -k', k, -k')$ in Equation 23, will need to vary as k^2 in order that the acoustic-mode frequency in Equation 27 will equal zero at $\mathbf{k} = 0$. Moreover, the order parameter will not necessarily be of the same symmetry as the corresponding normal-mode coordinate, because strain is the derivative of the atomic displacements rather than the actual displacements, so that α_k in Equation 37 will not be the same as $V_4(k, -k', k, -k')$. Taking account of these small modifications allows the basic model to apply also to soft acoustic modes. We will find in the next section that the behavior of the critical fluctuations depends on whether the soft mode is an optic mode or an acoustic mode.

THE RIGID UNIT MODE PICTURE OF DISPLACIVE PHASE TRANSITIONS IN SILICATES

In an attempt to take the theory of phase transitions further, recent work has focused on the central role of the rigidity of the SiO_4 (or AlO_4) tetrahedra in aluminosilicates (Dove et al. 1991, 1992a, 1996b; Dove 1997; Giddy et al. 1993; Hammonds et al. 1996). The phase transition in quartz is one example, where the rotations of tetrahedra lower the symmetry from hexagonal to trigonal (Grimm and Dorner 1975; Berge et al. 1986; Vallade et al. 1992). The polyhedral-tilting model (Megaw 1973; Hazen and Finger 1982) provides a geometric description of the phase transition. The development of this idea into the rigid-unit mode model involves identification of a low-frequency phonon mode that propagates with the movement of the SiO_4 (and AlO_4) tetrahedra as rigid units with no distortions (Hammonds et al. 1996). This rigid-unit mode (RUM) is a natural soft mode for the phase transition (Dove et al. 1995; Hammonds et al. 1996).

This last statement is more powerful than it appears at first, because the existence of any RUMs at all in a framework silicate is not trivial. In a simple mechanical structure, such as a framework structure made of loosely jointed tetrahedra, the number of possible modes of deformation is simply equal to the difference between the

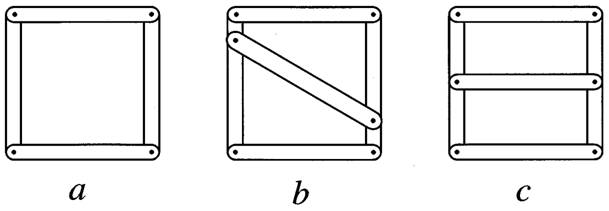

FIGURE 14. Illustration of how different arrangements of rods with cross bracing can allow for the existence of easy modes of deformation. Each rod has three degrees of freedom, and each linkage has two constraint equations. In arrangement (**a**) there are 12 degrees of freedom and 8 constraints. The difference of 4 includes the trivial two translations and the rotation of the whole object, and the shear deformation of the structure. In arrangement (**b**) there are 15 degrees of freedom and 12 constraints. The difference of 3 includes only the trivial two translations and the rotation of the whole object; there is now no possible shear deformation. Using the same simple counting arrangement (**c**) appears to have the same number of degrees of freedom and constraints as arrangement (**b**), but when the middle rod is parallel to the two horizontal rods we know that the object can be sheared as in arrangement (**a**). This deformation is allowed because the middle rod is controlled by only three constraints, two that tie one end onto the vertical rod, and the third that sets the orientation of the rod to be parallel to the other horizontal rods. Thus the number of independent constraints is 11.

total number of degrees of freedom, F, and the total number of constraints, C. Each tetrahedron has six degrees of freedom. Each corner has three constraint equations that links it to the corner of the connected tetrahedron, so the number of constraints per tetrahedron is also six. Thus the framework structure made of connected tetrahedra appears to be exactly constrained with $F = C$, and hence should have no modes of deformation. The fault in this reasoning is that symmetry can make some of the constraints redundant, so that there is a slightly lower number of independent constraints than the number of degrees of freedom. This principle is illustrated in Figure 14, where we show several two-dimensional arrangements of linked rods with constraints acting at the linkages. For a square of rods linked at corners and cross-braced by a fifth rod, the balance between the constraints and degrees of freedom allows only for uniform translations and rotations of the arrangements. However, if the fifth rod is parallel to two others, the two constraints that act at one end of this rod can be replaced by a single constraint that the rod should remain parallel to two others. This reduction in the total number of constraints then gives back to the structure one more degree of freedom, which in this case is the same shear deformation that would occur if the fifth rod was not in place. The more-detailed examples of two-dimensional frameworks of linked triangles and squares are given elsewhere (Dove et al. 1996c; Dove 1997). The fact that some deformation modes, which are equivalent to the RUMs in a framework silicate, can exist in a structure answers the question posed earlier of why phase transitions are allowed in a framework aluminosilicate crystal. The RUMs play the role of the soft modes in displacive phase transitions.

Giddy et al. (1993) and Hammonds et al. (1994) have developed a computational method to determine all RUMs for a given framework structure, taking account of all possible wave vectors. The basic idea is very simple. Each tetrahedron is viewed as a separate rigid body, and the atoms that are shared by two tetrahedra are counted as two separate atoms called split atoms. Any mode of deformation in which the rigid tetrahedra rotate and translate without causing the split atoms to separate is equivalent to a RUM in a framework silicate, and in this sense the separation of the split atoms plays the same role as the distortion of the tetrahedra. This way of thinking about the structure is easily incorporated into the formalism of molecular lattice dynamics (Pawley 1972; Dove 1993, Chapter 6). The RUMs are then the vibrational modes calculated to have zero frequency. Our computer program CRUSH (Hammonds et al. 1994) is freely available on the World Wide Web (http://www.esc.cam.ac.uk/mineral_sciences/crush.html). We have found that the number of RUMs in any structure is usually small compared to the total number of wave vectors, but significantly non-zero (Hammonds et al. 1996). Usually RUMs are confined to wave vectors that lie along lines or on planes in reciprocal space, but sometimes they exist on curved surfaces. We give some examples in Table 1. In our calculations with the constraints that the tetrahedra are perfectly rigid, and with no intertetrahedral forces, the RUMs are the modes with zero frequency. In reality the intertetrahedral forces will be non-zero, and these will lead to an energy spectrum for the RUMs. Inelastic neutron scattering experiments on leucite (Boysen 1990) and cristobalite (Swainson and Dove 1993a) give a range of RUM energies of the order of 0–1 THz (Dove et al. 1995). RUMs have been found by electron diffraction measurements from tridymite (Withers et al. 1994; Dove et al. 1996b) and cristobalite (Hua et al. 1988; Welberry et al. 1989; Withers et al. 1989), where their presence results in streaks of diffuse scattering corresponding to the intersections of the planes of the diffraction patterns with the planes of RUMs.

Implications of the rigid-unit mode model for displacive phase transitions

The idea of a RUM-driven phase transition is most easily illustrated with a model of a two-dimensional perovskite structure as represented in Figure 15. We first consider the high-symmetry phase, where the squares are initially aligned as in Figure 15a. If two neighboring squares rotate by angles φ_1 and φ_2, as in Figure 15b, we can write the energy to lowest order as (Dove et al. 1991, 1992a, 1995)

$$V(\varphi_1, \varphi_2) = \frac{1}{2}K(\varphi_1 + \varphi_2)^2. \tag{56}$$

This form expresses the fact that the only rotations that do not involve distortions of the squares, and thus are

TABLE 1. Numbers of rigid unit modes for symmetry points in the Brillouin zones of some aluminosilicates, excluding the trivial acoustic modes at **k** = 0

k	Quartz *P*6$_2$22	Cristo-balite *Fd*3*m*	Tridy-mite *P*6$_3$/*mmc*	Sanidine *C*2/*m*	Leucite *Ia*3*d*	Cordi-erite *Cccm*
(0,0,0)	1*(0)	3(1)	6*	0	5*(0)	6
(0,0,½)	3(1)	—	6	1*	—	6
(½,0,0)	2(1)	—	3*	—	—	6
(⅓,⅓,0)	1(1)	—	1	—	—	6
(⅓,⅓,½)	1(1)	—	2	—	—	0
(½,0,½)	1(1)	—	2	—	4(0)	2
(0,1,0)	—	2*	—	1	—	—
(½,½,½)	—	3(0)	—	0	0	—
(0,1,½)	—	—	—	1	—	—
(0,0,ξ)	3(0)	2(0)	6	—	0	6
(0,ξ,0)	2*(0)	2(2)	3	1	0	6
(ξ,ξ,0)	1(1)	1(0)	1	—	4(0)	6
(ξ,ξ,ξ)	—	3(0)	—	—	0	—
(½,0,ξ)	1(0)	—	2	—	0	2
(ξ,ξ,½)	1(1)	—	0	—	0	0
(½−ξ,2ξ,0)	1(1)	—	1	—	—	6
(½−ξ,2ξ,½)	1(1)	—	0	—	—	0
(0,ξ,½)	0(0)	—	1	1	—	—
(ξ,1,ξ)	—	1(0)	—	—	0	—
(ξ,ζ,0)	1(0)	0	1	—	0	6
(ξ,0,ζ)	0(0)	0	2	1	0	0
(ξ,1,ζ)	—	0	—	1	0	—
(ξ,ξ,ζ)	0(0)	1(0)	0	—	0	0

Note: Data from Hammonds et al. (1996). An * indicates a RUM that acts as the soft mode for a displacive instability in either the parent structure or a related structure. The "—" indicates that the wave vector is not of special symmetry in the particular structure. The numbers in brackets denote the numbers of RUMs that remain in the low-temperature phases.

relatively in low energy, are $\varphi_1 = -\varphi_2$. This is the distortion shown in Figure 15b. On the other hand, the greatest distortions of the squares are required when $\varphi_1 = \varphi_2$, which will lead to the greatest energy. The force constant K can be interpreted as the force required to distort the squares, the stiffness of the units.

We can now develop this argument further. Consider a three-dimensional framework of connected tetrahedra (or octahedra). For simplicity we subsume all the rigid-body motions of a tetrahedron into one parameter j, and note that when two neighboring units move together without distorting we can say that $\varphi_1 = -\varphi_2$. The energy of the full framework is given as

$$V_1 = \frac{1}{2}K \sum_{i,j}(\varphi_i + \varphi_j)^2$$

$$= K \sum_i \varphi_i^2 + K \sum_{i,j} \varphi_i\varphi_j. \quad (57)$$

It will become clear shortly why this is written in two forms, as with Equation 2. The energy as written contains no forces either to encourage or discourage the rotations of the tetrahedra; it simply provides the energy that encourages the tetrahedra to move in concert so as to avoid any distortions. First note that in general the high-temperature phases are fully expanded, with the phase transition involving a reduction in volume. In general the long-range dispersive interactions involving the highly polarizable O anions provide an inward pressure that attempts to reduce the volume; I develop this idea later. For the moment, I can express the effects of this inward pressure as the following energy:

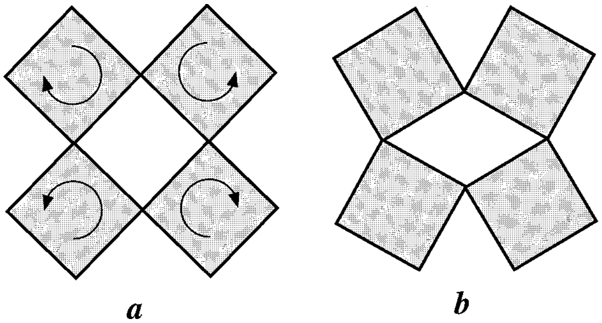

FIGURE 15. The only deformation pattern of an array of corner linked squares that does not require any distortion of the squares. (**a**) shows the ideal high-symmetry phase. (**b**) shows the distorted low-symmetry phase.

$$V_2 = -\mathcal{P} \sum_i \varphi_i^2. \quad (58)$$

Any given structure cannot collapse indefinitely. Either neighboring O atoms get too close, or there is a collapse of a cavity about a cation that eventually inhibits further collapse. These effects lead to short-range repulsive forces. The harmonic parts are subsumed within the parameters K and P. However, short-range steric forces have a strong anharmonic component, so we can simply write the short-range energy as a lowest-order anharmonic energy:

$$V_3 = \beta \sum_i \varphi_i^4. \quad (59)$$

This also includes the higher-order terms neglected in the expansion of Equation 56. When we add together these three contributions, we obtain (Dove et al. 1991, 1992a, 1995)

$$V = V_1 + V_2 + V_3 = \sum_i \{(K - \mathcal{P})\varphi_i^2 + \beta\varphi_i^4\}$$

$$+ K \sum_{i,j} \varphi_i\varphi_j. \quad (60)$$

The important point to note is that this is exactly analogous to the standard paradigm as expressed in Equation 2, where K plays the same role as J, and $\mathcal{P}$ and β play the parts of κ_2 and κ_4. Actually the signs of the last terms are different, but this is not important as it simply expresses the fact that in the standard paradigm two neighboring atoms want to move the same way whereas in this model two neighboring tetrahedra will rotate in opposite senses. By identifying K with the high stiffness of the tetrahedra, and $\mathcal{P}$ with the weak internal pressure due to the long-range dispersive interactions, we note that the model lies in the limit $K \gg \mathcal{P}$, which is equivalent to the displacive limit. This then provides a natural explanation for the fact that many phase transitions in silicates appear to behave as in the displacive limit and are accurately described by Landau theory.

We can follow further the analogy between the simple RUM model as represented by Equation 60 and the standard paradigm. The transition temperature for the standard paradigm has been given by Equations 8 and 34. From the analogy we find that the transition temperature is directly determined by *K*, the stiffness of the tetrahedra:

$$k_B T_c \propto K\mathcal{P}/\beta = K\varphi_0^2 \tag{61}$$

where φ_0 is the rotation of the tetrahedra at 0 K. This equation does not include prefactors (of order unity) that account for the detailed structure topology, which arise from the average of $J_{\mathbf{k}}^{-1}$ as in Equation 34. We have recently performed a calculation for quartz using a realistic value for *K* and taking account of all topological factors, and we found that it leads to a value of the transition temperature that is reasonably close to the experimental value (Dove et al. 1995).

It seems paradoxical that the transition temperature is determined by the stiffness of the tetrahedra when the soft mode is a RUM that does not involve any distortion of the tetrahedra. The point is that the vibrational entropy comes from all the other phonons, whose frequencies in the simple model are determined by *K* acting as a force constant. The behavior of the phonons was previously demonstrated in Figure 10, where ω^2 changes uniformly for all phonons. The transition temperature in the general case, Equation 46, is determined by the ratio of the average ω^2 to the shift in ω,^{2} which is determined by the single anharmonic coefficient β.

In this simple approach, we have considered the behavior of only one phonon branch, namely that which contains the soft mode, and we have quietly neglected all the other phonon branches. Are these neglected phonon branches important? The general equation for the transition temperature, Equations 28 and 46, involves contributions from all phonons, not just those on the branch containing the soft mode. However, lattice dynamics calculations for quartz (Dove 1995) have shown that the contribution to the thermodynamic functions from the complete set of phonons are largely self-canceling. Using the nomenclature of Equation 46, it was found that the mean value of α_k is substantially lower than the magnitudes of the individual values of α_k, but there is a wide spread of positive and negative values of α_k. From Equation 46 we see that $T_c \propto \langle\alpha_k\rangle^{-1}$. If $\langle\alpha_k\rangle$ is very small, values of T_c could be extremely large (because $\langle\alpha_k\rangle$ involves averaging over large positive and negative terms, its value is not well constrained), and we come again to an earlier question of why isn't $T_c \sim \infty$. We are rescued by the branch containing the soft mode. Within the quasiharmonic approximation this branch is uncoupled from the other phonon branches and can be described by the standard paradigm. As noted in this section, the anharmonic behavior of this branch is determined by the anharmonic coefficient β that operates equally for all wave vectors. Thus for this branch the mean value $\langle\alpha_k\rangle = \beta$ will not vanish, so that T_c will have a finite (i.e., controlled) value.

The origin of the driving force for phase transitions

Earlier I noted that there are two aspects to the driving forces for displacive phase transitions in silicates. First, there is the coupling between neighboring atoms that allows long-range ordering, described by the parameter *J* in the standard paradigm. Second there is a longer-range force that drives the actual deformation, which is described by the double-well potential, $V(\eta)$. The first aspect, which involves coupling between local ordering or deformation, has now been dealt with: It arises from the stiffness of the tetrahedra that leads to a local deformation propagating over large distances. We now consider the origin of the double-well potential $V(\eta)$. There are three contributions to $V(\eta)$ (Dove et al. 1995). First is the effect of long-range interactions, which some preliminary calculations (unpublished) have suggested are due to the dispersive interactions between the highly polarizable O atoms. The long-range interactions are attractive and pull the structure in to the highest density possible. Generally high-temperature phases have structures of maximum volume, and any RUM distortion leads to a lowering of the volume. The structure will collapse until halted by short-range repulsive interactions. The second contribution to $V(\eta)$ is the short-range attraction between a cation, such as K^+ or Ca^{2+}, which occupies a large cavity site, and neighboring O anions. These interactions may lead to a collapse of the cavity about the cation, which will propagate over large distance. This collapse is limited by the size of the cation. The third contribution to $V(\eta)$ arises from the energy associated with the Si-O-Si bond angle (either Si could also be Al). This has an ideal value of $\sim$145°, and bonds with angles that differ from this will have a higher energy. In some materials like cristobalite, the high-temperature phase appears to have a bond angle of 180° (Schmahl et al. 1992). In reality this will lead to a degree of disorder with neighboring tetrahedra rotating to try and reduce this angle (Swainson and Dove 1995), but in order for as many bonds as possible to have the ideal bond angle the structure must undergo the displacive phase transition. Thus in cristobalite the energy associated with the Si-O-Si bond angle contributes to $V(\eta)$ as a driving force for ordering. On the other hand, there are cases where the Si-O-Si bond angle is already near its ideal value in the high-temperature phase, so the energy associated with this bond will either oppose the phase transition, coming in to $V(\eta)$ with opposite sign to the first two contributions, or else the phase transition will involve the RUM distortion with the smallest distortion of the Si-O-Si bond angle (Dove et al. 1995).

These three contributions to $V(\eta)$ help to determine which of the potential phase transitions actually occurs. For example, in the high-temperature phase of quartz the Si-O-Si bond angle is already close to its ideal value, and only a few of the RUM distortions require no change in this angle. Leucite is like quartz in having the Si-O-Si bond angle close to its ideal value in the high-temperature phase. In this case the bond angle is changed by the all the RUM distortions, but the RUMs that are associated with the phase transition are those for which the changes in the bond angle are smallest (Dove et al. 1995b).

Critical fluctuations

Frequently, the temperature dependence of the order parameter follows the form of Equation 15, rather than the more general form of Equation 20 with $\beta < \frac{1}{2}$. The case $\beta = \frac{1}{2}$ occurs for mean-field theories, which are characterized by the existence of long-range ordering interactions. In our standard paradigm, the soft mode falls to zero frequency at a single wave vector. The range of interactions can be expressed by the correlation function

$$\langle Q(r)Q(0)\rangle = \int \langle Q_{\mathbf{k}}Q_{-\mathbf{k}}\rangle \exp(i\mathbf{k}\cdot\mathbf{r})d\mathbf{k} \qquad (62)$$

which has been written in terms of a Fourier transform relationship. The correlation function defines the range over which two local distortions of the form of the phonon eigenvector are correlated. For the purposes of a phase transition at $\mathbf{k} = 0$ (actually the arguments hold whatever wave vector the soft mode has), we can write $Q_{\mathbf{k}=0} = \eta$. Using Equation 24 for $\langle Q_{\mathbf{k}}Q_{-\mathbf{k}}\rangle$ Equation 62 can be written as

$$\langle Q(r)Q(0)\rangle = k_B T \int \omega_{\mathbf{k}}^{-2} \exp(i\mathbf{k}\cdot\mathbf{r})d\mathbf{k}. \qquad (63)$$

The standard paradigm has, for small wave vector, the form

$$\omega_{\mathbf{k}}^2 \approx \omega_0^2 + \alpha J|\mathbf{k}|^2 \qquad (64)$$

where α has the dimensions of length and reflects the interatomic spacing. Equation 64 is an expression of the fact that $\omega_{\mathbf{k}}$ has a minimum value at $k = 0$. Substitution of Equation 64 into Equation 63 gives the correlation function:

$$\langle Q(r)Q(0)\rangle \propto \frac{k_B T}{\omega_0^2} \int \frac{1}{1 + \xi^2 k^2} \exp(i\mathbf{k}\cdot\mathbf{r})d\mathbf{k} \qquad (65)$$

where ξ acts as a correlation length, defining the range of interactions:

$$\xi^2 = \alpha J/\omega_0^2. \qquad (66)$$

The Fourier transform yields

$$\langle Q(r)Q(0)\rangle \propto \frac{k_B T}{\xi^2 \omega_0^2 r} \exp(-r/\xi). \qquad (67)$$

We note two things. First, the inverse of the correlation length, ξ^{-1}, scales as $\omega_0 \propto (T - T_c)^{1/2}$, so that ξ diverges on cooling toward the transition temperature, in accord with standard results for mean-field theories (Bruce and Cowley 1981; Bruce and Wallace 1989; Yeomans 1992; Chaikin and Lubensky 1995). Second, the correlation length scales with J. This is the important result in the present discussion. Because J is identified with the stiffness of the tetrahedra, which we know to be large, we can immediately identify the origin of the long-range interactions and the reason that mean-field theory may be appropriate for displacive phase transitions in framework silicates.

We have not, however, taken account of any possible anisotropy of $\langle Q_{\mathbf{k}}Q_{-\mathbf{k}}\rangle$ in reciprocal space, or equivalently of $\omega_{\mathbf{k}}$. In our analysis we have assumed that $\omega_{\mathbf{k}}$ rises with $\mathbf{k}$ more-or-less equally for all directions of the wave vector in reciprocal space. The same RUM model that explains why J, and hence ξ, is large also suggests that the assumption of isotropy of $\langle Q_{\mathbf{k}}Q_{-\mathbf{k}}\rangle$ may be invalid (Sollich et al. 1994). In many cases the soft mode is part of a line or plane of RUMs in reciprocal space (Hammonds et al. 1996, Table 1). This is illustrated for perovskites such as $SrTiO_3$, (Fig. 2). The TiO_6 octahedra in one plane rotate in concert as in the two-dimensional example shown in Figure 15. The octahedra in the next plane up also undergo similar rotations, because the common vertices of octahedra between neighboring planes do not move. However, the octahedra in the next plane up can rotate in the same sense or opposite sense to the first plane. In fact from the point of view of the energy it really doesn't matter which way the next plane rotates. The only force operating will be an anharmonic interaction, mediated by the strain ($\propto 1 - \langle \cos\theta\rangle$, θ is the rotation angle) induced within a plane when the octahedra rotate, that tries to make the magnitude of the neighboring rotations, but not the signs, equal. Thus there is a strong correlation of rotations within each plane, but only a weak correlation between planes. Experimentally this is seen as a relatively flat phonon branch for wave vectors along the ⟨100⟩ directions connecting the zone-boundary wave vectors of the types {½½0} and {½½½} (Stirling 1972). For the specific examples of the octahedral-rotation phase transitions in the perovskites, Sollich et al. (1994) showed that this anisotropy is important and leads to departures of the temperature dependence of the order parameter from the Landau-form over the temperature range $\sim 0.9T_c \leq T \leq T_c$. Whether this anisotropy is important depends on the balance of two factors. The first factor is the degree of displaciveness (see Equation 5), which effectively defines how steeply the soft-mode frequency rises with wave vector on moving away from the critical wave vector along a hard direction compared to the square of the imaginary frequency of the soft mode. The second factor is the variation of frequency along the RUM branch containing the soft mode. This factor is more important if the RUM branch is on a plane of wave vectors rather than on a line of wave vectors. The balance between these factors has been quantified numerically, where the range of temperatures over which the form $\eta \propto (T_c - T)^{1/2}$ breaks down (defining the Ginzburg interval) was evaluated as a function of the two factors. Unfortunately because of a lack of experimental data for silicates, the size of the Ginzburg interval for quartz and cristobalite could only be guessed, and the guesses probably do not have any firm basis (Sollich et al. 1994).

The above arguments hold true when the soft mode is an optic phonon. When the soft mode is an acoustic phonon, with a softening of an elastic constant, the argument is rather different but more definitive. It has been shown that when the soft mode is an acoustic mode with the softening being restricted to specific directions only, mean-field theory is exactly correct in three dimensions (Cowley 1976; Folk et al. 1976, 1979; Bruce and Cowley 1981). This is the case for almost every second-order ferroelastic phase transition. When the acoustic modes soften for a plane of wave vectors the situation is more complicated. In three dimensions, deviations from Landau theory arise only as logarithmic corrections and in practice are extremely difficult to observe. More dramatic is the prediction (Mayer and Cowley 1988), recently confirmed for the only known example of a second-order ferroelastic phase transition with planar softening of the acoustic modes, Na_2CO_3 (Harris et al. 1993, 1995, 1996; Harris and Dove 1995; Swainson et al. 1995), that at the transition the mean-square atomic displacements should diverge and long-range order completely lost.

The nature of high-temperature phases

We noted earlier that several possible models exist for the nature of the high-temperature phases. The contrast of $PbTiO_3$ and $BaTiO_3$ is relatively simple to envision. In $BaTiO_3$ the positions of the Ti^{4+} cations are disordered, and this disorder shows up by an overdamping of the soft mode (Yamada et al. 1969; Harada et al. 1971). On the other hand, in $PbTiO_3$ the ions simply vibrate about their average positions, and the soft mode is underdamped (Shirane et al. 1970; Burns and Scott 1970). Thus locally the structure of $BaTiO_3$ looks similar to that of the low-temperature phase on the scale of the unit-cell size, albeit with dynamic switching between different orientations of the polar direction, whereas the local structure of $PbTiO_3$ looks like the average structure with the ions vibrating about their mean positions.

The controversies arise when we consider the nature of the high-temperature phases of silicates such as quartz and cristobalite, leaving aside for the moment more complicated aluminosilicates such as leucite and anorthite. In the high-temperature phase of cristobalite the average structure deduced from diffraction studies has a linear Si-O-Si bond (Schmahl et al. 1992). Because it was established both by energy calculations (Lasaga and Gibbs 1987, 1988; Gibbs et al. 1994) and by comparison with other silicates that linear bonds are energetically unfavorable compared to bonds with an angle of around 145°, it has been suggested that there must be some degree of disorder in the high-temperature phase. For example, the Si-O bonds may be tilted at an angle to the $\langle 111 \rangle$ directions, but their orientations about these directions must be disordered to be consistent with the crystal symmetry. Recent measurements of the total neutron scattering intensity from β-cristobalite (Dove 1997, and unpublished results) yielded a radial distribution function consistent with an average Si-O-Si angle of around 145°. The problems come when attempts are made to produce a model that gives this local structure. Si-O bonds are not independent entities, but are part of the SiO_4 tetrahedra that are tightly bound. Therefore the motion of one Si-O bond will be strongly coupled to the motion of connected Si-O bonds.

In the case of β-cristobalite two models have been proposed that are based on the existence of domains of lower symmetry structures (Wright and Leadbetter 1975; Hatch and Ghose 1991). Similar models have also been proposed for quartz, but in this case the need for a disordered high-temperature phase seems less clear (Salje et al. 1992). Part of the appeal of domain models is that they provide the means of accounting for disorder of the orientations of the Si-O bonds and the correlations between connected Si-O bonds at the same time. Any distortions of the tetrahedra only occur within the walls between domains. The RUM model provides a way of building up a domain wall with only a minimum amount of distortion of the tetrahedra. If RUMs exist over a line or plane of wave vectors, it will be possible to construct a linear combination of RUM distortions as a Fourier summation over all wave vectors, leading to a distortion pattern in real space (Swainson and Dove 1993b; Hammonds et al. 1996; Dove et al. 1996c). This distortion pattern could be a set of domains with domain walls. But if there is enough freedom in the Fourier summation, the sizes of the domains and the sizes of the domain walls could be arbitrary without significant distortions of the tetrahedra. Thus the RUM model allows the distinct domains to evaporate, leaving a dynamically disordered phase that is generated by a superposition of many large-amplitude RUM phonons. For β-cristobalite the RUM picture with dynamic disorder rather than domains has received some support from light scattering (Swainson and Dove 1993a) and molecular dynamics simulations (Swainson and Dove 1995).

Part of the problem with understanding the nature of the high-temperature phases has been the lack of relevant experimental data. There has been very little inelastic neutron scattering work on these problems. Several phase transitions in silicates were studied using NMR (Phillips et al. 1992, 1993; Phillips and Kirkpatrick 1995; Kirkpatrick 1988; Spearing et al. 1992, 1994; Stebbins 1988), but NMR probes a frequency range (typically only up to the MHz regime) below that of the dynamics of atoms (around the THz regime). Raman and infrared spectroscopy are useful tools (Iqbal and Owens 1984; Salje 1992b), because they probe the THz frequency regime and are sensitive to short-range correlations (Salje 1992b). For the phase transitions in quartz and cristobalite, the spectral lines that are expected to vanish in the high-symmetry phase, if there are no domains present, actually do so (Salje et al. 1992; Swainson and Dove 1993a). This suggests that the domain models are not good models for the nature of the high-temperature phases of these materials.

EXPERIMENTAL REALIZATION

Simple displacive phase transitions

It is expected that the theory reviewed above should be directly applicable to the displacive phase transitions in minerals such as quartz, albite, anorthite, and leucite. In these examples the Si-O-Si bond angles in the high-temperature phases are around 145°, so there will be no orientational disorder of the tetrahedra in the high-temperature phases. The case of quartz has been documented in some detail. Indeed, the soft mode in the low-temperature phase quartz was the first ever soft mode to be observed experimentally (Raman and Nedungadi 1940), and although a lattice dynamic interpretation followed soon after (Saksena 1940), it was another twenty years before the soft-mode model was properly formulated. The soft mode has since been measured in more detail in both phases by spectroscopy (Shapiro et al. 1967; Scott 1974; Tezuka et al. 1991) and inelastic neutron scattering (Dolino et al. 1992), in relation to both the α-β phase transition and the incommensurate instability. The soft-mode model appears to be appropriate for quartz, and the incommensurate phase transition is naturally explained by the RUM model (Berge et al. 1986; Bethke et al. 1987, Tautz et al. 1991; Vallade et al. 1992). This work in quartz has been reviewed in detail by Dolino and Vallade (1992).

Unfortunately there have been hardly any other reported attempts to measure soft modes or RUM spectra in other silicates. In part this is because such measurements would require a major undertaking. The number of phonon branches in a complicated silicate is large, meaning that to disentangle the phonon spectra is not easy. Moreover, because the vibrational energy will be shared between all phonon modes, the amplitude of any one phonon mode, and hence the intensity of the neutron beam scattering from that phonon mode, will be relatively weak. To make matters even more difficult, it is quite likely that at temperatures close to the transition temperature the soft mode will be damped (see the results for quartz reviewed by Dolino and Vallade 1994). One system for which preliminary data have been reported is leucite (Boysen 1990). Tentative low-frequency phonon dispersion curves have been proposed. These lend support to the RUM model of the phase transition in leucite, by showing the soft phonons involved in the phase transition (Dove et al. 1995). The soft modes in the low-temperature phase of cristobalite have been measured by spectroscopy (Swainson and Dove, unpublished), but in this case the phase transition is so discontinuous that the softening of the phonon frequencies on approaching the transition temperature is not very large.

Order-disorder phase transitions in silicates

The theory reviewed in this article is relevant for cases in which the entropy is mostly vibrational rather than configurational. How do the ideas apply to a material such as cristobalite, where the linear Si-O-Si bonds given by the average structure of the high-temperature phase lead to a disordered structure in which neighboring tetrahedra are tilted with respect to each other? The order-disorder phase transitions can arise as an opposite extreme to displacive phase transitions, where atoms hop between two potential minima. The example used is the ordering of the Ti^{4+} cations in $BaTiO_3$. In the disordered phase the Ti^{4+} cations can occupy one of the eight $\langle 111 \rangle$ sites. The entropy could be deduced from simple configurational counting considerations as in the spin-½ Ising model. On the other hand, in cristobalite the orientation of any tetrahedra is constrained by the orientations of the neighboring tetrahedra. If we recast the disorder into Fourier space, the disorder of the Ti^{4+} cations in $BaTiO_3$ can be decomposed into Fourier components from all wave vectors. In cristobalite, the disorder arises from superpositions of RUMs of phonons that lie in planes of wave vectors rather than over all reciprocal space. Therefore it is quite likely that the entropy from the orientational disorder in cristobalite is not large compared with the vibrational entropy from all the other phonons that we have considered in this review article. This point however has not yet been quantified; it is one of the open questions that we leave with this article.

Al-Si ordering in aluminosilicates

A more common type of order-disorder phase transition involves the ordering of different cations, for example the ordering of Al and Si framework cations in aluminosilicates. The simplest theoretical approach is the Bragg-Williams model. The ordering energies can be expressed in terms of an Ising model, Equation 6, where J is the energy required to form two Al-O-Si linkages from the linkages Si-O-Si and Al-O-Al. The entropy that drives the disordering at high temperatures is assumed to be configurational, Equation 55. In the simplest model with equal numbers of both cations, the free energy is given by

$$\begin{aligned} G &= -4J\eta^2 + \mathrm{R}T[(1+\eta)\ln(1+\eta) \\ &\quad + (1-\eta)\ln(1-\eta)] \\ &\approx -4J\eta^2 + \mathrm{R}T(\eta^2 + \eta^4/6 + \cdots). \end{aligned} \tag{68}$$

Calculations have shown that J typically lies in the range 60–100 kJ/mol (Thayaparam et al. 1994, 1996; Dove et al. 1996a).

For comparison I have performed some calculations (unpublished) of the phonon spectra of cordierite with both complete order and disorder appropriate for the high-temperature phase (the T1 sites have Al occupancy of ⅔, and the T2 sites have occupancy of ⅓), using the models described by Winkler et al. (1991). The resultant entropy leads to an additional term

$$G_{\text{phonon}} = \mu \mathrm{R} T \eta^2 \tag{69}$$

where μ has the value 0.1 (for energy per mole of tetrahedra). This is to be compared with a total entropy change from $\eta = 0$ to $\eta = 1$ of 0.64R per mole of tetrahedra, assuming that the disorder is completely random. In practice the entropy change will be less than this, because the configurations favored in the disordered phase are those that minimize the total number of Al-O-Al linkages. The phonon entropy is not as large as the configurational entropy, but it is not insignificant in comparison. The quantitative details are still an open issue.

Orientational ordering phase transitions

The classic example of an orientational order-disorder phase transition in a mineral is in calcite. Above 1260 K the carbonate molecular ions become disordered with respect to orientations about their three-fold axes (Dove and Powell 1989; Dove et al. 1992b, 1997; Hagen et al. 1992). Specifically, in the disordered phase each carbonate ion will flip between orientations that are related by a rotation of 60° (equivalent to 180°). It might be imagined that this model looks like a simple order-disorder case, with the ordering driven by nearest-neighbor orientational interactions and the disorder driven by configuration entropy involving two possible orientations of each carbonate ion. However, the structural investigations performed on heating up to the phase transition reveal a quite different picture. Instead the orientational disorder is driven by large amplitude librations of the carbonate ions (Markgraf and Reeder 1985; Dove et al. 1997). The disorder sets in when the librational amplitude approaches 30°, when the carbonate ions are no longer confined to the ordering potential. Fourier maps of the nuclear density show that there is a negligible population of the disordered orientations until very close to the phase transition, far less than would be expected in a classical order-disorder phase transition (Markgraf and Reeder 1985; Dove et al. 1997). Calculations of the rotational ordering potential similar to Equation (1) indicate that the parameter s corresponding to Equation 5 is of order unity (Dove et al. 1997). Thus the phase transition in calcite is mid-way between the order-disorder and displacive limits (Padlewski et al. 1992). Therefore, there is significant entropy that comes from the effect of the ordering on the phonons rather than from the configurational disorder. This behavior was also found in a molecular dynamics simulation (Ferrario et al. 1994). The quantitative details are still an open issue.

First-order phase transitions

The theory developed in this article is easily applied to second-order phase transitions. By an appropriate choice of $V(\eta)$, Equation 36, the theory can be applied to first-order phase transitions. In this section it is worth airing the question of whether a first-order phase transition simply follows from the form of $V(\eta)$, or whether there is something more significant to the fact of a phase transition being first-order. From renormalization group theory it is known that some phase transitions must be first-order (Bruce and Cowley 1981). Actually this statement is in principle stronger than it might seem at first. Any phase transition in which there is a coupling of the order parameter to strain must be first order on the basis of renormalization group theory (the so-called strain-induced first-order phase transitions; Bruce and Cowley 1981). This is not the same as the origin of a first order discontinuity from strain coupling in the sense of Landau theory, but arises from more subtle considerations. However, the size of the first-order step is likely to be so small as to be virtually unobservable. There are also other possible causes of first-order discontinuities that arise in renormalization group theory, but again the size of the effect is not known. Cristobalite is an interesting example (Schmahl et al. 1992). There is a large discontinuity at the transition temperature, and it is clear that this does not arise from the strain coupling in the Landau free energy. The quantitative treatment of the origin of first-order discontinuities in phase transitions is an open question.

Phase transitions at high pressures

The theory we have developed is strictly only applicable to phase transitions that occur on changing temperature. It is tempting to tinker with the basic theory to incorporate the effects of pressure. For example, a term of the form PV could be added to the free energy, noting that the change in volume at a phase transition usually scales as $\Delta V \propto -\eta^2$. When this term is included in the Landau free energy expansion, Equation 13, there is a correction to the term that is quadratic in η leading to a subsequent change in the transition temperature on changing pressure, i.e.,

$$G(\eta) = \frac{1}{2}a(T - T_c)\eta^2 + \cdots - \frac{1}{2}\gamma P\eta^2 \qquad (70)$$

which gives the renormalized transition temperature

$$T_c^* = T_c + \gamma P/a. \qquad (71)$$

This approach, however, is not likely to lead to a quantitatively self-consistent model. The problem with changing pressure is that it always produces a volume change. The models we have described in this article have assumed that any changes of volume (or, more generally, to changes of the structure), aside from those associated with the phase transition, are negligible. The effect of this is that parameters such as κ_2, κ_4, ω_k and α_k, which we used earlier, can be assumed to be more-or-less independent of temperature. This assumption is usually reasonable. However, on increasing pressure it is probable that the values of all these parameters will change significantly. Although at any fixed pressure the theory we have developed here is directly applicable, we cannot simply take that theory and apply it for a fixed temperature with changing pressure. What we need is a quantitatively founded (rather than empirical) model for how the basic parameters to change with pressure; this is our final open question of this article.

One thing we might expect is that on increasing pressure the value of η^2 at 0 K will increase. In a silicate, it is more likely that the structure will crumple than the tetrahedra will distort (at least for moderate pressures). In this case, we expect in the application of Equation 61 for the transition temperature that K, the stiffness of the tetrahedra, will not significantly change with pressure (at least in the limit of low pressures), whereas φ_0 will increase on increasing pressure, leading to a transition temperature that will increase on increasing pressure. This is the common case. The pressure dependence of φ_0 will directly reflect the pressure-dependence of κ_2 and κ_4. On the other hand, the case of anorthite is different, with $\mathrm{d}T_c/\mathrm{d}P < 0$ (Hackwell and Angel 1995). We do not know the reason for this, but part of the explanation may lie in the fact that the structure can distort with no change in symmetry relatively easily, which may lead to a hardening of the potential opposing ordering of φ_0 (Hammonds et al. 1996). This has not yet been quantified.

The effect of pressure may be even more complicated. When we associate the soft mode with a RUM of the high-symmetry phase, we usually neglect the fact that there are other RUMs that could be alternative soft modes. With each RUM there will be an associated set of κ_2, κ_4, ω_k, and α_k. At a fixed pressure, only one set will give the minimum free energy, and all other sets can be safely forgotten (more commonly, they are not even known). However, on increasing pressure the free energy associated with the RUM that acts as the soft mode at low pressures may become less significant than the free energy associated with another RUM. In this case there could be a phase transition with increasing pressure between two phases that are daughter structures of the same high-symmetry phase, even though the symmetry of one of the two lower-symmetry structures appears to be a subgroup of the symmetry of the other one. An example of this is cristobalite. The α-β phase transition involves a RUM distortion of the high-temperature β phase that plays the role of a soft mode (Swainson and Dove 1993a). The high-pressure phase (Palmer and Finger 1994) can also be viewed as a RUM deformation of the β phase (Hammonds et al. 1996). However, the high-pressure phase cannot be derived from the α phase by a RUM distortion (Hammonds et al. 1996). This means that there will be a potential energy barrier between the α phase and the high-pressure phase, and it is probable that one should really think about the high-pressure phase in relation to the β phase rather than in relation to the α phase, even though on increasing pressure at ambient temperature the transition involves a change from the α phase to the high-pressure phase.

Computational studies of displacive phase transitions

Finally, it is worth noting that computational methods are playing an increasingly important role in the study of displacive phase transitions. At one level, simple empirical models can be used to determine the dominant transition mechanism, as in studies of the phase transitions in leucite (Dove et al. 1993) and the alkali and calcium and strontium feldspars (Dove and Redfern 1997). These calculations can be particularly useful for answering well-specified questions, even though simple energy calculations cannot properly incorporate the effects of temperature. One of the problems with empirical potentials is that they are optimized against crystal structures, elastic constants, and phonon frequencies, but not against absolute energies, so it may not be possible to calculate the relevant energies (e.g., the potential $V(\eta)$ of Equation 36) with adequate accuracy. As computer power increases, the way around this problem is to use first-principles quantum mechanical calculations. These methods have been used to good effect in determining the transition mechanisms in the ferroelectric perovskites through calculations of the potential energy wells (Cohen and Krakauer 1992; Inbar and Cohen 1996), but applications to mineralogical problems are presently few. An exception is the study of possible phase transitions in $MgSiO_3$ perovskite by Warren and Ackland (1996). Both empirical and first-principles methods can, at least in principle, be used to calculate the coeffecients ω_k and α_k in Equation 46. This was done for quartz (Dove et al. 1995, and unpublished); an earlier calculation for $SrTiO_3$ was carried out by Bruce and Cowley (1973).

To incorporate temperature it is necessary to use Monte Carlo or molecular dynamics methods. Recently first-principles methods have been used to calculate effective interatomic potentials for ferroelectric perovskites for use in Monte Carlo (Zhong et al. 1994, 1995) and molecular dynamics (Gong and Cohen 1992) calculations of transition temperatures. A number of molecular dynamics simulations of phase transitions in minerals have been reported (e.g., Tsuneyuki et al. 1988; Tautz et al. 1991; Ferrario et al. 1994; Swainson and Dove 1995). Very few simulations have been concerned with calculations of the phonon spectra beyond the density of states, although the methods to extract phonon dispersion curves from molecular dynamics are well established (e.g., Dove 1993, Chapter 12). Tautz et al. (1991) calculated the phonon spectra for quartz from a large molecular dynamics simulation to obtain the fundamental parameters for the theory of the incommensurate phase transition. It is hoped that these methods will play an increasingly decisive role in linking the theory of phase transitions to specific case studies. However, it is essential that these simulations are large enough. Small samples may have only a few wave vectors that are essential for the phase transition. For example, if a high-temperature phase is formed of a dynamic superposition of RUMs of many wave vectors, and the simulation only contains a few wave vectors, it is likely that this would significantly alter the structure of the high-temperature phase in the simulation. The simulated high-temperature phase may actually be forced by the finite size to look like that suggested by the domain models, and caution should be used when citing the results of molecular dynamics simulations using small samples in support of any particular interpretation.

CONCLUSIONS

In this review, I have posed a number of questions that arise from the existence of phase transitions in minerals, and I have attempted to answer some of them. In some respects the underlying physics of the phase transitions in minerals is no different from that of other materials, and it is perfectly reasonable to apply standard theories to them. But by bringing the stiffness of the SiO_4 and AlO_4 tetrahedra into the theory, we have been able to provide some physical content to the theory, and place some constraints on the behavior. A number of open questions have been identified.

One of the aims of this review is to encourage further quantitative studies of displacive phase transitions in minerals. One technique that could be usefully applied to these studies is inelastic neutron scattering. This technique has been applied in a few cases, and the success of these studies will hopefully spur further efforts.

Finally, I remarked earlier that the displacive phase transitions in minerals may give new insights that are of value outside of mineralogy. The RUM model can be extended to non-silicates, and in these cases the corresponding version of the theory will also explain why a given phase transition might be consistent with the displacive limit. The essential feature will be that certain bond lengths or contact distances should be nearly rigid. For example, in close-packed ionic crystals with hard short-range repulsive interactions, atoms in contact will move by sliding around each other rather than by squashing into each other. Thus the possible patterns of deformation are limited to the set in which the contact distances remain constant. Examples are the ferroelastic phase transitions in Na_2CO_3 and the molecular system HCN (Dove et al. 1992a). The strong short-range forces play the same role as the stiffness of the SiO_4 tetrahedra in determining the displacive limit.

ACKNOWLEDGMENTS

This work has partly been supported by EPSRC and NERC (UK). Part of this article was written while the author was a visitor to Chalk River Laboratories (Atomic Energy of Canada Limited), whose staff are thanked for their kind hospitality. I am indebted to colleagues (now or previously) in Cambridge, Volker Heine, Kenton Hammonds, Andrew Giddy, Peter Sollich, Ekhard Salje, Ian Swainson, and Simon Redfern, for many discussions about displacive phase transitions in minerals. I would also like to thank David Palmer for the use of his CrystalMaker program to produce the crystal structure diagrams. This article is dedicated to my wife Kate and daughters Jennifer-Anne, Emma-Clare, and Mary-Ellen.

REFERENCES CITED

Axe, J.D. (1971) Neutron studies of displacive phase transitions. Transactions of the American Crystallographic Association, 7, 89–103.

Bauer, M., and Klee, W.E. (1993) The monoclinic hexagonal phase transition in chlorapatite. European Journal of Mineralogy, 5, 307–316.

Bell, A.M.T., Cernik, R.J., Champness, P.E., Fitch, A.N., Henderson, C.M.B., Kohn, S.C., Norledge, B.V., and Redfern, S.A.T. (1993) Crystal structures of leucites from synchrotron X-ray powder diffraction data. Materials Science Forum, 133–136, 697–702.

Bell, A.M.T., Henderson, C.M.B., Redfern, S.A.T., Cernik, R.J., Champness, P.E., Fitch, A.N., and Kohn, S.C. (1994) Structures of synthetic $K_2MgSi_5O_{12}$ leucites by integrated x-ray powder diffraction, electron diffraction and ^{29}Si MAS NMR methods. Acta Crystallographica, B50, 31–41.

Berge, B., Bachheimer, J. P., Dolino, G., Vallade, M., and Zeyen, C.M.E. (1986) Inelastic neutron scattering study of quartz near the incommensurate phase transition. Ferroelectrics, 66, 73–84.

Bethke, J., Dolino, G., Eckold, G., Berge, B., Vallade, M., Zeyen, C.M.E., Hahn, T., Arnold, H., and Moussa, F. (1987) Phonon dispersion and mode coupling in high-quartz near the incommensurate phase transition. Europhysics Letters, 3, 207–212.

Bismayer, U., Schmahl, W., Schmidt, C., and Groat, L.A. (1992) Linear birefringence and x-ray diffraction studies of the structural phase transition in titanite, $CaTiSiO_5$. Physics and Chemistry of Minerals, 19, 260–266.

Blinc, R., and Zeks, B. (1974) Soft Modes in Ferroelectrics and Antiferroelectrics. North Holland (Amsterdam).

Boeriogoates, J., Artman, J.I., and Woodfield, B.F. (1990) Heat capacity studies of phase transitions in langbeinites. 2. $K_2Mg_2(SO_4)_3$. Physics and Chemistry of Minerals, 17, 173–178.

Boysen, H. (1990) Neutron scattering and phase transitions in leucite. In Salje, E.K.H., Ed., Phase Transitions In Ferroelastic And Co-Elastic Crystals, p. 334–349. Cambridge University Press, Cambridge.

Brown, N.E., Ross, C.R., and Webb, S.L. (1994) Atomic displacements in the normal incommensurate phase transition in Co-Åkermanite ($Ca_2CoSi_2O_7$). Physics and Chemistry of Minerals, 21, 469–480.

Bruce, A. D., and Cowley, R.A. (1981) Structural Phase Transitions. Taylor and Francis, London.

Bruce, A. D., and Wallace, D.J. (1989) Critical point phenomena: universal physics at large length scales. In Davies, P., Ed., The New Physics. Cambridge University Press (Cambridge)

Burns, G., and Scott, B.A. (1970) Raman studies of underdamped soft modes in $PbTiO_3$. Physical Review Letters, 25, 167–170.

Capobianco, C., and Carpenter, M.A. (1989) Thermally induced changes in kalsilite, ($KAlSiO_4$). American Mineralogist, 74, 797–811.

Catti, M., Ferraris, G., Hull, S., and Pavese, A. (1995) Static compression and H-disorder in brucite, $Mg(OH)_2$, to 11 GPa: a powder neutron diffraction study. Physics and Chemistry of Minerals, 22, 200–206.

Castex, J., and Madon, M. (1995) Test of the vibrational modelling for the λ-type transitions: application to the α–β quartz transition. Physics and Chemistry of Minerals, 22, 1–10.

Cellai, D., Carpenter, M.A., and Heaney, P.J. (1992) Phase transitions and microstructures in natural kaliophilite. European Journal of Mineralogy, 4, 1209–1220.

Cellai, D., Carpenter, M.A., Wruck, B., and Salje, E.K.H. (1994) Characterization of high temperature phase transitions in single crystals of steinbach tridymite. American Mineralogist, 79, 606–614.

Cellai, D., Carpenter, M.A., Kirkpatrick, R.J., Salje, E.K.H., and Zhang, M. (1995) Thermally-induced phase transitions in tridymite: An infrared spectroscopy study. Physics and Chemistry of Minerals, 22, 50–60.

Chaikin, P.M., and Lubensky, T.C. (1995) Principles of Condensed Matter Physics. Cambridge University Press (Cambridge).

Cochran, W. (1959) Crystal stability and the theory of ferroelectricity. Physical Review Letters, 3, 412–414.

——— (1960) Crystal stability and the theory of ferroelectricity. Advances in Physics, 9, 387–423.

——— (1981) Soft modes, a personal perspective. Ferroelectrics, 35, 3–8.

Cohen, R.E., and Krakauer, H. (1992) Electronic structure studies of the differences in ferroelectric behavior of $BaTiO_3$ and $PbTiO_3$. Ferroelectrics, 136, 65–83.

Cowley, R.A. (1962) Temperature dependence of a transverse optic mode in strontium titanate. Physical Review Letters, 9, 159–161.

——— (1976) Acoustic phonon instabilities and structural phase transitions. Physical Review, B13, 4877–4885.

Cowley, R.A., Buyers, W.L., and Dolling, G. (1969) Relationship of normal modes of vibration of strontium titanate and its antiferroelectric phase transition at 110 K. Solid State Communications, 7, 181–184.

Daniel, I., Gillet, P., and Ghose, S. (1995) A new high-pressure phase transition in anorthite ($CaAl_2Si_2O_8$) revealed by Raman spectroscopy. American Mineralogist, 80, 645–648.

de Dombal, R.F., and Carpenter, M.A. (1993) High temperature phase transitions in Steinbach tridymite. European Journal of Mineralogy, 5, 607–622.

Depmeier, W. (1988) Aluminate sodalites a family with strained structures and ferroic phase transitions. Physics and Chemistry of Minerals, 15, 419–426.

——— (1992) Remarks on symmetries occurring in the sodalite family. Zeitschrift für Kristallographie,199, 75–89.

Depmeier, W., and Bührer, W. (1991) Aluminate Sodalites: $Sr_8[Al_{12}O_{24}](MoO_4)_2$ (SAM) at 293, 423, 523, 623 and 723 K and

$Sr_8[Al_{12}O_{24}](CrO_4)_2$ (SAW) at 293 K. Acta Crystallographica, B47, 197–206.

Devarajan, V., and Salje, E. (1986) Phase transitions in langbeinites. 2. Raman spectroscopic investigations of $K_2Cd_2(SO_4)_3$. Physics and Chemistry of Minerals, 13, 25–30.

Dolino, G. (1990) The α–inc–β transitions of quartz: A century of research on displacive phase transitions. Phase Transitions, 21, 59–72.

Dolino, G., and Vallade, M. (1994) Lattice dynamical behavior of anhydrous silica. Reviews in Mineralogy, 29, 403–431.

Dolino, G., Berge, B., Vallade, M., and Moussa, F. (1989) Inelastic neutron scattering study of the origin of the incommensurate phase of quartz. Physica, B156, 15–16.

——— (1992) Origin of the incommensurate phase of quartz: I. Inelastic neutron scattering study of the high temperature β phase of quartz. Journal de Physique, I. 2, 1461–1480.

Dorner, B., Ed., (1982) Coherent Inelastic Neutron Scattering in Lattice Dynamics. Springer–Verlag (Berlin).

Dorner, B., Boysen, H., Frey, F., and Grimm, H. (1981) On the Si–O–Si bond angle in α-quartz and β-quartz. Journal de Physique, 42, 752–754.

Dove, M.T. (1993) Introduction to Lattice Dynamics, 258p. Cambridge University Press, Cambridge.

Dove, M.T. (1997) Silicates and soft modes. In Amorphous Insulators and Semiconductors: Proceedings of NATO ASI, ed. Thorpe, M.F. and Mitkova, M.I. (Kluwer, Dordrecht, 349–383).

Dove, M.T., and Powell, B.M. (1989) Neutron diffraction study of the tricritical orientational order-disorder phase transition in calcite at 1260 K. Physics and Chemistry of Minerals, 16, 503–507.

Dove, M.T., and Redfern, S.A.T. (1997) Lattice simulation studies of the ferroelastic phase transitions in $(Na,K)AlSi_3O_8$ and $(Sr,Ca)Al_2Si_2O_8$ feldspar solid solutions. American Mineralogist, 82, 8–15.

Dove, M.T., Giddy, A.P., and Heine, V. (1991) Rigid unit mode model of displacive phase transitions in framework silicates. Transactions of the American Crystallographic Association, 27, 65–74.

——— (1992a) On the application of mean-field and Landau theory to displacive phase transitions. Ferroelectrics, 136, 33–49.

Dove, M.T., Hagen, M.E., Harris, M.J., Powell, B.M., Steigenberger, U., and Winkler, B. (1992b) Anomalous inelastic neutron scattering from calcite. Journal of Physics: Condensed Matter, 4, 2761–2774.

Dove, M.T., Winkler, B., Leslie, M., Harris, M.J., and Salje, E.K.H. (1992c) A new interatomic potential model for calcite: Applications to lattice dynamics studies, phase transition, and isotope fractionation. American Mineralogist, 77, 244–250.

Dove, M.T., Cool, T., Palmer, D.C., Putnis, A., Salje, E.K.H., and Winkler, B. (1993) On the role of Al-Si ordering in the cubic–tetragonal phase transition of leucite. American Mineralogist, 78, 486–492.

Dove, M.T., Heine, V., and Hammonds, K.D. (1995) Rigid unit modes in framework silicates. Mineralogical Magazine, 59, 629–639.

Dove, M.T., Thayaparam, S., Heine, V., and Hammonds, K.D. (1996a) The phenomenon of low Al/Si ordering temperatures in aluminosilicate framework structures. American Mineralogist, 81, 349–362.

Dove, M.T., Hammonds, K.D., Heine, V., Withers, R.L., Xiao, Y., and Kirkpatrick R.J. (1996b) Rigid Unit Modes in the High-Temperature Phase of SiO_2 Tridymite: Calculations and Electron Diffraction. Physics and Chemistry of Minerals, 23, 55–61.

Dove, M.T., Gambhir, M., Hammonds, K.D., Heine, V., and Pryde, A.K.A. (1996c) Distortions of framework structures. Phase Transitions 58, 121–143.

Dove, M.T., Swainson, I.P., Powell, B.M., and Tennant, D.C. (1997) Structural studies of the orientational order-disorder phase transition in calcite, $CaCO_3$. Physics and Chemistry of Minerals (in press).

Duffy, T.S., Meade, C., Fei, Y., Mao, H.K., and Hemley, R.J. (1995) High-pressure phase-transition in brucite, $Mg(OH)_2$. American Mineralogist, 80, 222–230.

Ferrario, M., Lynden-Bell, R.M., Mcdonald, I.R. (1994) Structural fluctuations and the order-disorder phase-transition in calcite. Journal of Physics: Condensed Matter, 6, 1345–1358.

Fiquet, G., Guyot, F., and Itie, J.P. (1994) High-pressure X-ray diffraction study of carbonates: $MgCO_3$, $CaMg(CO_3)_2$, and $CaCO_3$. American Mineralogist, 79, 15–23.

Fleury, P.A., Scott, J.F., and Worlock, J.M. (1968) Soft phonon modes and the 110 K phase transition in $SrTiO_3$. Physical Review Letters, 21, 16–19.

Folk, R., Iro, H., and Schwabl, F. (1976) Critical statics of elastic phase transitions. Zeitschrift für Physik, B25, 69.

——— (1979) Critical dynamics of elastic phase transitions. Physical Review, B20, 1229.

Gallup, R.F., and Coleman, L.B. (1990) Vibrational spectra and the ferroelectric phase transition of colemanite. Physics and Chemistry of Minerals, 17, 271–274.

Ghazibayat, B., Behruzi, M., Litterst, F.J., Lottermoser, W., and Amthauer, G. (1992) Crystallographic phase transition and valence fluctuation in synthetic Mn-bearing ilvaite $CaFe^{2+}{}_{2}x Mn^{2+} x Fe^{3+}[Si_2O_7/O/(OH)]$. Physics and Chemistry of Minerals, 18, 491–496.

Ghose, S. (1985) Lattice dynamics, phase transitions and soft modes. Mineralogical Society of America Reviews in Mineralogy, 14, 127–163.

——— (1988) Inelastic neutron scattering. Mineralogical Society of America Reviews in Mineralogy, 18, 161–192.

Ghose, S., van Tendeloo, G., and Amelinckx, S. (1988) Dynamics of a 2nd-order phase transition: $P1$–$I\bar{1}$ phase transition in anorthite, $CaAl_2Si_2O_8$. Science, 242, 1539–1541.

Ghose, S., Tsukimura, K., and Hatch, D.M. (1989) Phase transitions in ilvaite, a mixed-valence iron silicate. 2. A single crystal x-ray diffraction study and Landau theory of the monoclinic to orthorhombic phase transition induced by charge delocalization. Physics and Chemistry of Minerals, 16, 483–496.

Ghose, S., Ito, Y., and Hatch, D.M. (1991) Paraelectric–antiferroelectric phase transition in titanite, $CaTiSiO_5$. 1. A high temperature x-ray diffraction study of the order parameter and transition mechanism. Physics and Chemistry of Minerals, 17, 591–603.

Ghose, S., McMmullan, R.K., and Weber, H.P. (1993) Neutron diffraction studies of the $P1$–$I1$ transition in anorthite, $CaAl_2Si_2O_8$, and the crystal structure of the body-centered phase at 514 K. Zeitschrift für Kristallographie, 204, 215–237.

Gibbs, G.V. (1966) The polymorphism of cordierite I: The crystal structure of low cordierite. American Mineralogist, 51, 1068–1087.

Gibbs, G.V., Downs, J.W., and Boisen Jr., M.B. (1994) The elusive SiO bond. Reviews in Mineralogy, 29, 331–368.

Giddy, A.P., Dove, M.T., and Heine, V. (1989) What does the Landau free energy really look like for structural phase transitions? Journal of Physics: Condensed Matter, 1, 8327–8335.

——— (1990) The non-analytic nature of Landau free energies. Ferroelectrics, 104, 331–335.

Giddy, A.P., Dove, M.T., Pawley, G.S., and Heine, V. (1993) The determination of rigid unit modes as potential soft modes for displacive phase transitions in framework crystal structures. Acta Crystallographica, A49, 697–703.

Gong, Z., and Cohen, R.E. (1992) Molecular dynamics study of $PbTiO_3$ using nonempirical potentials. Ferroelectrics, 136, 113–124.

Grimm, H., and Dorner, B. (1975) On the mechanism of the a–b phase transformation of quartz. Physics and Chemistry of Solids, 36, 407–413.

Güttler, B., Salje, E., and Ghose, S. (1989a) Polarized single-crystal absorption-spectroscopy of the P*nam*–*P*2$_1$/*a* transition of ilvaite $Ca(Fe^{2+},Fe^{3+})Fe^{2+}Si_2O_2(OH)$ as measured between 300 K and 450 K. Physics and Chemistry of Minerals, 16, 606–613.

Güttler, B., Salje, E., and Putnis, A. (1989b) Structural states of Mg-cordierite. 3. Infrared spectroscopy and the nature of the hexagonal-modulated transition. Physics and Chemistry of Minerals, 16, 365–373.

Guyot, F., Richet, P., Courtial, P., and Gillet, P. (1993) High temperature heat capacity and phase transitions of $CaTiO_3$ perovskite. Physics and Chemistry of Minerals, 20, 141–146.

Hackwell, T.P., and Angel, R.J. (1995) Reversed brackets for the $P\bar{1}$–$I\bar{1}$ transition in anorthite at high pressures and temperatures. American Mineralogist, 80, 239–246.

Hagen, M., Dove, M.T., Harris, M.J., Steigenberger, U., and Powell, B.M. (1992) Orientational order-disorder phase transition in calcite. Physica, B180–181, 276–278.

Hammonds, K.D., Dove, M.T., Giddy, A.P., and Heine, V. (1994) Crush: A Fortran program for the analysis of the rigid unit mode spectrum of a framework structure. American Mineralogist, 79, 1207–1209.

Hammonds, K.D., Dove, M.T., Giddy, A.P., Heine, V., and Winkler, B. (1996) Rigid unit phonon modes and structural phase transitions in framework silicates. American Mineralogist, 81, 1057–1079.

Harada, J., Axe, J.D., and Shirane, G. (1971) Neutron scattering study of soft modes in cubic $BaTiO_3$. Physical Review, B4, 155–162.

Harris, M.J., and Dove, M.T. (1995) Lattice Melting at Structural Phase Transitions. Modern Physics Letters, B9, 67–85.

Harris, M.J., Salje, E.K.H., Güttler, B.K., and Carpenter, M.A. (1989) Structural states of natural potassium-feldspar: An infrared spectroscopic study. Physics and Chemistry of Minerals, 16, 649–658.

Harris, M.J., Salje, E.K.H., and Güttler, B.K. (1990) An infrared spectroscopic study of the internal-modes of sodium nitrate: Implications for the structural phase transition. Journal Of Physics: Condensed Matter, 2, 5517–5527.

Harris, M.J., R A Cowley, Swainson, I.P., and Dove, M.T. (1993) Observation of lattice melting at the ferroelastic phase transition in Na_2CO_3. Physical Review Letters, 71, 2939–2942.

Harris, M.J., Dove, M.T., and Godfrey, K.W. (1995) Observation of lattice melting in a single crystal: The ferroelastic phase transition in Na_2CO_3. Physical Review, 51, 6758–6760.

——— (1996) A single crystal neutron scattering study of lattice melting in ferroelastic Na_2CO_3. Journal of Physics: Condensed Matter, 8, 7075–7084.

Hatch, D.M., and Ghose, S. (1989a) A dynamical model for the $I\overline{1}$–$P\overline{1}$ phase transition in anorthite, $CaAl_2Si_2O_8$. 2. Order parameter treatment. Physics and Chemistry of Minerals, 16, 614–620.

——— (1989b) Symmetry analysis of the phase transition and twinning in $MgSiO_3$ garnet: Implications to mantle mineralogy. American Mineralogist, 74, 1221–1224.

——— (1991) The α–β phase transition in cristobalite, SiO_2: Symmetry analysis, domain structure, and the dynamic nature of the β-phase. Physics and Chemistry of Minerals, 17, 554–562.

Hatch, D.M., and Merrill, L. (1981) Landau description of the calcite–CaCO3 (II) phase transition. Journal of Chemical Physics, 23, 368–374.

Hatch, D.M., and Griffen, D.T. (1989) Phase transitions in the grandite garnets. American Mineralogist, 74, 151–159.

Hatch, D.M., Artman, J.I., and Boeriogoates, J. (1990a) Phase transition in $K_2Cd_2(SO_4)_3$: Order parameter and microscopic distortions. Physics and Chemistry of Minerals, 17, 334–343.

Hatch, D.M., Ghose, S., and Stokes, H.T. (1990b) Phase transitions in leucite, $KAlSi_2O_6$. 1. Symmetry analysis with order parameter treatment and the resulting microscopic distortions. Physics and Chemistry of Minerals, 17, 220–227.

Hawthorne, F.C., Ungaretti, L., Oberti, R., Caucia, F., and Callegari, A. (1993) The crystal chemistry of staurolite. 2. Order-disorder and the monoclinic–orthorhombic phase transition. Canadian Mineralogist, 31, 583–595.

Hazen, R.M., and Finger, L.W. (1982) Comparative crystal chemistry: temperature, pressure, composition and the variation of crystal structure. Wiley, Chichester.

——— (1983) High pressure and high temperature crystallographic study of the gillespite I–II phase transition. American Mineralogist, 68, 595–603.

Heaney, P.J. (1994) Structure and chemistry of the low-pressure silica polymorphs. Reviews in Mineralogy, 29, 1–40.

Heaney, P.J., and Veblen, D.R. (1990) A high temperature study of the low–high leucite phase transition using the transmission electron microscope. American Mineralogist, 75, 464–476.

——— (1991) Observations of the α–β phase transition in quartz: A review of imaging and diffraction studies and some new results. American Mineralogist, 76, 1018–1032.

Hemingway, B.S., Evans, H.T., Nord, G.L., Haselton, H.T., Robie, R.A., and McGee, J.J. (1986) Åkermanite phase transitions in heat capacity and thermal expansion, and revised thermodynamic data. Canadian Mineralogist, 24, 425–434.

Hemley, R.J., Prewitt, C.T., and Kingma, K.J. (1994) High-pressure behavior of silica. Reviews in Mineralogy, 29, 41–81.

Hua, G.L., Welberry, T.R., Withers, R.L., and Thompson, J.G. (1988) An electron diffraction and lattice-dynamical study of the diffuse scattering in β-cristobalite, SiO_2. Journal of Applied Crystallography, 21, 458–465.

Hugh-Jones, D.A., Woodland, A.B., and Angel, R.J. (1994) The structure of high-pressure *C2 / c* ferrosilite and crystal chemistry of high-pressure *C2 / c* pyroxenes. American Mineralogist, 79, 1032–1041.

Inbar, I., and Cohen, R.E. (1996) Comparison of the electronic structures and energetics of ferroelectric $LiNbO_3$ and $LiTaO_3$. Physical Review B53, 1193–1204.

Iqbal, Z., and Owens, F.J., Eds. (1984) Vibrational Spectroscopy of Phase Transitions. Academic Press (Orlando).

Ito, Y., Kuehner, S., and Ghose, S. (1991) Phase transitions in leucite determined by high-temperature, single-crystal x-ray diffraction. Zeitschrift für Kristallographie, 197, 75–84.

Kan, X.M., Ghose, S., and Dunlap, B.D. (1988) Phase transitions in ilvaite, a mixed valence iron silicate.1. A Fe-57 Mössbauer study of magnetic order and spin frustration. Physics and Chemistry of Minerals, 16, 55–60.

Kihara, K. (1978) Thermal change in unit-cell dimensions, and a hexagonal structure of tridymite. Zeitschrift für Kristallographie, 148, 237–253.

——— (1995) Disorder and successive structure transitions in the tridymite forms of SiO_2. Physics and Chemistry of Minerals, 22, 223–232.

Kirkpatrick, R.J. (1988) MAS NMR-spectroscopy of minerals and glasses. Reviews in Mineralogy, 18, 341–403.

Lange, R.A., Carmichael, I.S.E., and Stebbins, J.F. (1986) Phase transitions in leucite ($KAlSi_2O_6$), orthorhombic $KAlSiO_4$, and their iron analogs ($KFeSi_2O_6$, $KFeSiO_4$). American Mineralogist, 71, 937–945.

Lasaga, A.C., and Gibbs, G.V. (1987) Applications of quantum mechanical potential surfaces to mineral physics calculations. Physics and Chemistry of Minerals, 14, 107–117.

——— (1988) Quantum mechanical potential surfaces and calculations on minerals and molecular clusters. Physics and Chemistry of Minerals, 16, 29–41.

Lefebvre, J., Fouret, R., and Zeyen, C.M.E. (1984) Structure determination of sodium nitrate near the order-disorder phase transition. Journal de Physique, 45, 1317–1327.

Li, Z., Chan, S.K., and Ghose, S. (1990) Elastic properties of the incommensurate phase of Åkermanite, $Ca_2MgSi_2O_7$. Physics and Chemistry of Minerals, 17, 462–466.

Lines, M.E., and Glass, A.M. (1977) Principles and Applications of Ferroelectrics and Related Materials. Clarendon Press (Oxford).

Liu, L.G., and Mernagh, T.P. (1990) Phase transitions and Raman spectra of calcite at high pressures and room temperature. American Mineralogist, 75, 801–806.

Lyddane, R.H., Sachs, R.G., and Teller, E. (1941) On the polar vibrations of alkali halides. Physical Review, 59, 673–676.

Markgraf, S.A., and Reeder, R.J. (1985) High-temperature structure refinements of calcite and magnesite. American Mineralogist, 70, 590–600.

Mayer, A.P., and Cowley, R.A. (1988) The continuous melting transition of a 3-dimensional crystal at a planar elastic instability. Journal of Physics C: Solid State Physics, 21, 4827–4834.

McGuinn, M.D., and Redfern, S.A.T. (1994a) Ferroelastic phase transition in $SrAl_2Si_2O_8$ feldspar at elevated pressure. Mineralogical Magazine, 58, 21–26.

——— (1994b) Ferroelastic phase transition along the join $CaAl_2Si_2O_8$–$SrAl_2Si_2O_8$. American Mineralogist, 79, 24–30.

Meagher, E.P., and Gibbs, G.V. (1977) The polymorphism of cordierite II: The crystal structure of indialite. Canadian Mineralogist, 15, 43–49.

Megaw, H.D. (1973) Crystal structures: a working approach. W.B. Saunders, Philadelphia.

Merrill, L., and Basset, W.A. (1975) The crystal structure of CaCO3 (II), a high-pressure metastable phase of calcium carbonate. Acta Crystallographica, B31, 343–349.

Merwin, L.H., Sebald, A., and Seifert, F. (1989) The incommensurate–commensurate phase transition in åkermanite, $Ca_2MgSi_2O_7$, observed by *in situ* Si-29 MAS NMR spectroscopy. Physics and Chemistry of Minerals, 16, 752–756.

Miyake, M., and Iwai, S. (1981) Phase transition of potassium sulfate,

K_2SO_4. 3. Thermodynamical and phenomenological study. Physics and Chemistry of Minerals, 7, 211–215.

Miyake, M., Matsuo, M., Hata, M., and Iwai, S. (1981) Phase transition of potassium sulfate, K_2SO_4 (II) Dielectric constant and electrical conductivity. Physics and Chemistry of Minerals, 7, 88–90.

Padlewski, S., Evans, A.K., Ayling, C., and Heine, V. (1992) Crossover between displacive and order-disorder behavior in the F^4 model. Journal of Physics: Condensed Matter, 4, 4895–4908.

Palmer, D.C. (1994) Stuffed derivatives of the silica polymorphs. Reviews in Mineralogy, 29, 83–122.

Palmer, D.C., and Salje, E.K.H. (1990) Phase transitions in leucite: Dielectric properties and transition mechanism. Physics and Chemistry of Minerals, 17, 444–452.

Palmer, D.C., and Finger, L.W. (1994) Pressure induced phase transition in cristobalite: An x-ray powder diffraction study to 4.4 GPa. American Mineralogist, 79, 1–8.

Palmer, D.C., Salje, E.K.H., and Schmahl, W.W. (1989) Phase transitions in leucite: X-ray diffraction studies. Physics and Chemistry of Minerals, 16, 714–719.

Palmer, D.C., Bismayer, U., and Salje, E.K.H. (1990) Phase transitions in leucite: Order parameter behavior and the Landau potential deduced from Raman spectroscopy and birefringence studies. Physics and Chemistry of Minerals, 17, 259–265.

Palmer, D.C., Hemley, R.J., and Prewitt, C.T. (1994) Raman spectroscopic study of high pressure phase transitions in cristobalite. Physics and Chemistry of Minerals, 21, 481–488.

Palmer, D.C., Dove, M.T., Ibberson, R.M., and Powell, B.M. (1997) Structural behavior, crystal chemistry and phase transitions in substituted leucites: high-resolution neutron powder diffraction studies. American Mineralogist, 82, 16–30.

Pawley, G.S. (1972) Analytic formulation of molecular lattice dynamics based on pair potentials. Physica Status Solidi, 49b, 475–488.

Phillips, B.L., and Kirkpatrick, R.J. (1995) High-temperature Si-29 MAS NMR spectroscopy of anorthite ($CaAl_2Si_2O_8$) and its $P\bar{1}$–$I\bar{1}$ structural phase transition. Physics and Chemistry of Minerals, 22, 268–276.

Phillips, B.L., Kirkpatrick, R.J., and Carpenter, M.A. (1992) Investigation of short-range Al,Si order in synthetic anorthite by Si-29 MAS NMR-spectroscopy. American Mineralogist, 77, 484–494.

Phillips, B.L., Thompson, J.G., Xiao, Y., and Kirkpatrick, R.J. (1993) Constraints on the structure and dynamics of the β-cristobalite polymorphs of SiO_2 and $AlPO_4$ from ^{31}P, ^{27}Al and ^{29}Si NMR spectroscopy from 770 K. Physics and Chemistry of Minerals, 20, 341–352.

Poon, W.C.-K., Putnis, A., Salje, E. (1990) Structural states of Mg-cordierite. 4. Raman spectroscopy and local order parameter behavior. Journal of Physics: Condensed Matter, 2, 6361–6372.

Putnis, A. (1992) Introduction to Mineral Sciences. Cambridge University Press, Cambridge.

Putnis, A., Salje, E., Redfern, S.A.T., Fyfe, C.A., and Stobl, H. (1987) Structural states of Mg-cordierite I: Order parameters from synchrotron X-ray and NMR data. Physics and Chemistry of Minerals, 14, 446–454.

Percival, M.J.L. (1990) Optical absorption spectroscopy of doped materials: The $P2_13$–$P2_12_12_1$ phase transition in $K_2(Cd_{0.98}Co_{0.02})_2(SO_4)_3$. Mineralogical Magazine, 54, 525–535.

Percival, M.J.L., Schmahl, W.W., and Salje, E. (1989) Structure of cobalt doped $K_2Cd_2(SO_4)_3$ langbeinite at 3 temperatures above the $P2_13$–$P2_12_12_1$ phase transition, and a new trigger mechanism for the ferroelastic transformation. Physics and Chemistry of Minerals, 16, 569–575.

Radescu, S., Etxebarria, I., Perez-Mato, J.M. (1995) The Landau free-energy of the 3-dimensional Φ^4 model in wide temperature intervals. Journal of Physics: Condensed Matter, 7, 585–595.

Raman, C.V., and Nedungadi, T.M.K. (1940) The α–β transformation of quartz. Nature, 145, 147.

Redfern, S.A.T. (1992) The effect of Al/Si disorder on the $I\bar{1}$–$P\bar{1}$ co-elastic phase transition in Ca-rich plagioclase. Physics and Chemistry of Minerals, 19, 246–254.

——— (1993) Hard-mode infrared study of the ferroelastic phase-transition in $CuWO_4$–$ZnWO_4$ mixed crystals. Physical Review, B48, 5761–5765.

——— (1996) High-temperature structural phase transition in perovskite ($CaTiO_3$). Journal of Physics: Condensed Matter, 8, 8267–8270.

Redfern, S.A.T., and Salje, E. (1987) Thermodynamics of plagioclase. 2. Temperature evolution of the spontaneous strain at the $I\bar{1}$–$P\bar{1}$ phase transition in anorthite. Physics and Chemistry of Minerals, 14, 189–195.

——— (1992) Microscopic dynamic and macroscopic thermodynamic character of the $I\bar{1}$–$P\bar{1}$ phase transition in anorthite. Physics and Chemistry of Minerals, 18, 526–533.

Redfern, S.A.T., Graeme-Barber, A., and Salje, E. (1988) Thermodynamics of plagioclase III: Spontaneous strain at the $I\bar{1}$–$P\bar{1}$ phase transition in Ca-rich plagioclase. Physics and Chemistry of Minerals, 16, 157–163.

Redfern, S.A.T., Salje, E., Maresch, W., and Schreyer, W. (1989a) X-ray powder diffraction and infrared study of the hexagonal to orthorhombic phase transition in K-bearing cordierite. American Mineralogist, 74, 1293–1299.

Redfern, S.A.T., Salje, E., and Navrotsky, A. (1989b) High temperature enthalpy at the orientational order disorder transition in calcite: Implications for the calcite aragonite phase equilibrium Contributions to Mineralogy and Petrology, 101, 479–484.

Redfern, S.A.T., Clark, S.M., and Henderson, C.M.B. (1993) High pressure phase transition in gillespite: new evidence from energy-dispersive diffraction. Materials Research Forum 133–136, 615–620.

Redfern, S.A.T., Bell, A.M.T., Henderson, C.M.B., and Schofield, P.F. (1995) Rietveld study of the structural phase-transition in the sanmartinite ($ZnWO_4$)–cuproscheelite ($CuWO_4$) solid solution. European Journal of Mineralogy, 7, 1019–1028.

Redfern, S.A.T., McGuinn, M.D., Clark, S.M., and Henderson, C.M.B. (1997) High-pressure ferroelastic and coelastic behaviour at the orthorhombic-tetragonal phase transition in gillespite. Mineralogical Magazine (in press)

Reeder, R.J., Redfern, S.A.T., and Salje, E. (1988) Spontaneous strain at the structural phase transition in $NaNO_3$. Physics and Chemistry of Minerals, 15, 605–611.

Rothlisberger, F., Seifert, F., and Czank, M. (1990) Chemical control of the commensurate–incommensurate phase transition in synthetic melilites. European Journal of Mineralogy, 2, 585–594.

Saksena, B.D. (1940) Analysis of the Raman and infrared spectra of a-quartz. Indian Academy of Sciences, A12, 93–139.

Salje, E. (1986) Raman spectroscopic investigation of the order parameter behavior in hypersolvus alkali feldspar displacive phase transition and evidence for Na–K site ordering. Physics and Chemistry of Minerals, 13, 340–346.

——— (1987) Thermodynamics of plagioclases. 1. Theory of the $I\bar{1}$–$P\bar{1}$ phase transition in anorthite and Ca-rich plagioclases. Physics and Chemistry of Minerals, 14, 181–188.

Salje, E.K.H. (1990a) Phase transitions in ferroelastic and co-elastic crystals. Cambridge University Press, Cambridge.

Salje, E. (1990b) Phase-transitions in ferroelastic and co-elastic crystals. Ferroelectrics, 104, 111–120.

Salje, E.K.H. (1991a) Some aspects of the thermodynamic behavior of ferroelastic and co-elastic phase transitions. Phase Transitions, 34, 25–52.

Salje, E.K.H. (1991b) Crystallography and structural phase transitions, an introduction. Acta Crystallographica, A47, 453.

Salje, E.K.H. (1992a) Application of Landau theory for the analysis of phase transitions in minerals. Physics Reports, 215, 49–99.

Salje, E.K.H. (1992b) Hard mode spectroscopy: experimental studies of structural phase transitions. Phase Transitions, 37, 83–110.

Salje, E., and Wruck, B. (1991) Order parameter saturation at low-temperatures: Numerical results for displacive and O/D systems. Ferroelectrics, 124, 185–188.

Salje, E.K.H., Wruck, B., and Thomas, H. (1991) Order-parameter saturation and low-temperature extension of Landau theory. Zeitschrift fur Physik, B82, 399–404.

Salje, E.K.H., Ridgewell, A., Güttler, B., Wruck, B., Dove, M.T., and Dolino, G. (1992) On the displacive character of the phase transition in quartz: a hard mode spectroscopy study. Journal of Physics: Condensed Matter, 4, 571–577.

Salje, E., Schmidt, C., and Bismayer, U. (1993) Structural phase transition in titanite, $CaTiSiO_5$: A Raman spectroscopic study. Physics and Chemistry of Minerals, 19, 502–506.

Schmahl, W.W. (1993) Athermal transformation behavior and thermal hysteresis at the SiO_2 α/β cristobalite phase transition. European Journal of Mineralogy, 5, 377–380.

Schmahl, W.W., and Salje, E. (1989) X-ray diffraction study of the orientational order/disorder transition in NaNO3: Evidence for order parameter coupling. Physics and–Chemistry of Minerals, 16, 790–798.

Schmahl, W.W., Swainson, I.P., Dove, M.T., and Graeme-Barber, A. (1992) Landau free energy and order parameter behaviour of the α–β phase transition in cristobalite. Zeitschrift für Kristallographie, 201, 125–145.

Schofield, P.F., and Redfern, S.A.T. (1992) Ferroelastic phase transition in the sanmartinite ($ZnWO_4$)–cuproscheelite ($CuWO_4$) solid solution. Journal of Physics: Condensed Matter, 4, 375–388.

———(1993) Temperature-dependence and composition-dependence of the ferroelastic phase-transition in $(Cu\mathit{x}Zn_{1-}\mathit{x})WO_4$. Journal of Physics and Chemistry of Solids, 54, 161–170.

Schofield, P.F., Charnock, J.M., Cressey, G., and Henderson, C.M.B. (1994) An EXAFS study of cation site distortions through the $P2/c$ – $P\overline{1}$ transition in the synthetic cuproscheelite–sanmartinite solid solution. Mineralogical Magazine, 58, 185–199.

Scott, J.F. (1974) Soft mode spectroscopy: experimental studies of structural phase transitions. Reviews of Modern Physics, 46, 83–128.

Seifert, F., and Rothlisberger, F. (1993) Macroscopic and structural changes at the incommensurate–normal phase transition in melilites. Mineralogy and Petrology, 48, 179–192.

Shapiro, S.M., O'Shea, D.C., and Cummins, H.Z. (1967) Raman scattering study of the α–β phase transition in quartz. Physical Review Letters, 19, 361–364.

Shimobayashi, N., and Kitamura, M. (1991) Phase transition in Ca-poor clinopyroxenes: A high-temperature transmission electron microscopic study. Physics and Chemistry of Minerals, 18, 153–160.

Shirane, G. (1974) Neutron scattering studies of structural phase transitions at Brookhaven. Reviews of Modern Physics, 46, 437–449.

Shirane, G., and Yamada, Y. (1969) Lattice-dynamical study of the 110 K phase transition in $SrTiO_3$. Physical Review, 177, 858–863.

Shirane, G., Axe, J.D., Harada, J., and Remeika, J.P. (1970) Soft ferroelectric modes in lead titanate. Physical Review, B2, 155–159.

Skold, K., and Price, D.L., Eds., (1986) Neutron Scattering. Academic Press (Orlando).

Sollich, P., Heine, V., and Dove, M.T. (1994) The Ginzburg interval in soft mode phase transitions: Consequences of the Rigid Unit Mode picture. Journal of Physics: Condensed Matter, 6, 3171–3196.

Spearing, D.R., Farnan, I., and Stebbins, J.F. (1992) Dynamics of the α–β phase transitions in quartz and cristobalite as observed by in situ high temperature Si-29 NMR and O-17 NMR. Physics and Chemistry of Minerals, 19, 307–321.

Spearing, D.R., Stebbins, J.F., and Farnan, I. (1994) Diffusion and the dynamics of displacive phase transitions in cryolite (Na_3AlF_6) and chiolite ($Na_5Al_3F_{14}$): Multinuclear NMR studies. Physics and Chemistry of Minerals, 21, 373–386.

Speer, D., and Salje, E. (1986) Phase transitions in langbeinites. 1. Crystal chemistry and structures of K double sulfates of the langbeinite type $M_2K_2(SO_4)_3$, M = Mg, Ni, Co, Zn, Ca. Physics and Chemistry of Minerals, 13, 17–24.

Stebbins, J.F. (1988) NMR-spectroscopy and dynamic processes in mineralogy and geochemistry. Reviews in Mineralogy, 18, 405–429.

Stirling, W.G. (1972) Neutron inelastic scattering study of the lattice dynamics of strontium titanate: harmonic models. Journal of Physics, C: Solid State Physics, 5, 2711–2730.

Stokes, H. T., and Hatch, D.M. (1988) Isotropy Subgroups of the 230 Crystallographic Space Groups. World Scientific, Singapore.

Sueno, S., Prewitt, C.T., and Kimata, M. (1985) Structural aspects of phase transitions in Fe-Mg-Ca Pyroxenes. American Mineralogist, 70, 141–148.

Swainson, I.P., and Dove, M.T. (1993a) Low-frequency floppy modes in β-cristobalite. Physical Review Letters, 71, 193–196.

———(1993b) Comment on ''First-Principles Studies on Structural Properties of β-cristobalite. Physical Review Letters, 71, 3610.

———(1995) Molecular dynamics simulation of a- and β-cristobalite. Journal of Physics: Condensed Matter, 7, 1771–1788.

Swainson, I.P., Dove, M.T., and Harris, M.J. (1995) Neutron powder diffraction study of the ferroelastic phase transition in sodium carbonate. Journal of Physics: Condensed Matter Physics, 7, 4395–4417.

Tagai, T., Takeda, H., Tachikawa, O., Schropfer, L., Fuess, H., Kaminuma, H., and Kyle, P.R. (1988) Microstructure and phase transitions of Ca-rich anorthoclase. Neues Jahrbuch für Mineralogie Monatshefte, 9–20.

Tautz, F.S., Heine, V., Dove, M.T., and Chen, X.J. (1991) Rigid unit modes in the molecular dynamics simulation of quartz and the incommensurate phase transition. Physics and Chemistry of Minerals, 18, 326–336.

Tezuka, Y., Shin, S., and Ishigame, M. (1991) Observation of the silent soft mode in β-quartz by means of hyper-Raman scattering. Physical Review Letters, 66, 2356–2359.

Thayaparam, S., Dove, M.T., and Heine, V. (1994) A computer simulation study of Al/Si ordering in gehlenite and the paradox of the low transition temperature. Physics and Chemistry of Minerals, 21, 110–116.

Thayaparam, S., Heine, V., Dove, M.T., and Hammonds, K.D. (1996) A computational study of Al/Si ordering in cordierite. Physics and Chemistry of Minerals, 23, 127–139.

Thouless, D.J. (1989) Condensed matter physics in less than three dimensions. In, Davies, P., ed., The New Physics. Cambridge University Press (Cambridge)

Tribaudino, M., Benna, P., and Bruno, E. (1993) $I\overline{1}$–$I2/c$ phase transition in alkaline earth feldspars along the $CaAl_2Si_2O_8$–$SrAl_2Si_2O_8$ join: Thermodynamic behavior. Physics and Chemistry of Minerals, 20, 221–227.

Tsuneyuki, S., Tsukada, M., Aoki, H., and Matsui, Y. (1988) First principles interatomic potential of silica applied to molecular dynamics. Physical Review Letters, 61, 869–872.

Vallade, M., Berge, B., and Dolino, G. (1992) Origin of the incommensurate phase of quartz: II. Interpretation of inelastic neutron scattering data. Journal de Physique, I. 2, 1481–1495.

Van Tendeloo, G., Ghose, S., and Amelinckx, S. (1989) A dynamical model for the $P\overline{1}$–$I\overline{1}$ phase transition in anorthite, $CaAl_2Si_2O_8$. 1. Evidence from electron microscopy. Physics and Chemistry of Minerals, 16, 311–319.

Van Heurck, C., Van Tendeloo, G., Ghose, S., and Amelinckx, S. (1991) Paraelectric-antiferroelectric phase transition in titanite, $CaTiSiO_5$. 2. Electron diffraction and electron microscopic studies of the transition dynamics. Physics and Chemistry of Minerals, 17, 604–610.

Vogt, T., and Schmahl, W.W. (1993) The high-temperature phase-transition in perovskite. Europhysics Letters, 24, 281–285.

Warren, M.C., and Ackland, G.J. (1996) Ab initio studies of structural instabilities in magnesium silicate perovskite. Physics and Chemistry of Minerals, 23, 107–118.

Webb, S.L., Ross, C.R., and Liebertz, J. (1992) Thermal expansion and spontaneous strain associated with the normal incommensurate phase transition in melilites. Physics and Chemistry of Minerals, 18, 522–525.

Welberry, T.R., Hua, G.L., and Withers, R.L. (1989). An optical transform and Monte Carlo study of the disorder in β-cristobalite SiO_2. Journal of Applied Crystallography, 22, 87–95.

Wilson, C.C. (1994) Structural studies of schultenite in the temperature-range 125–324 K by pulsed single-crystal neutron diffraction: hydrogen ordering and structural distortions. Mineralogical Magazine, 58, 629–634.

Winkler, B., Dove, M.T., and Leslie, M. (1991) Static lattice energy minimization and lattice dynamics calculations on aluminosilicate minerals. American Mineralogist, 76, 313–331.

Withers, R.L., Thompson, J.G., and Welberry, T.R. (1989) The structure and microstructure of α-cristobalite and its relationship to β-cristobalite. Physics and Chemistry of Minerals, 16, 517–523.

Withers, R.L., Thompson, J.G., Xiao, Y., and Kirkpatrick, R.J. (1994) An electron diffraction study of the polymorphs of SiO_2-tridymite. Physics and Chemistry of Minerals, 21, 421–433.

Wright, A.F., and Leadbetter, A.J. (1975) The structures of the β-cristobalite phases of SiO_2 and $AlPO_4$. Philosophical Magazine, 31, 1391–1401.

Xiao, Y.H., Kirkpatrick, R.J., and Kim, Y.J. (1993) Structural phase transitions of tridymite: A ^{29}Si-MAS NMR investigation. American Mineralogist, 78, 241–244.

——— (1995a) Investigations of MX-1 tridymite by Si-29 MAS NMR: modulated structures and structural phase transitions. Physics and Chemistry of Minerals, 22, 30–40.

Xiao, Y.H., Kirkpatrick, R.J., Hay, R.L., Kim, Y.J., and Phillips, B.L. (1995b) Investigation of Al,Si order in K-feldspars using Al-27 and Si-29 MAS NMR. Mineralogical Magazine, 59, 47–61.

Yamada, Y., Shirane, G., and Linz, A. (1969) Study of critical fluctuations in $BaTiO_3$ by neutron scattering. Physical Review, 177, 848–857.

Yang, H.X., Ghose, S., and Hatch, D.M. (1993) Ferroelastic phase transition in cryolite, Na_3AlF_6, a mixed fluoride perovskite: high temperature single crystal x-ray diffraction study and symmetry analysis of the transition mechanism. Physics and Chemistry of Minerals, 19, 528–544.

Yeomans, J.M. (1992) Statistical mechanics of phase transitions. Clarendon Press (Oxford).

Zhang, M., Salje, E.K.H., Bismayer, U., Unruh, H.G., Wruck, B., and Schmidt, C. (1995) Phase transitions in titanite $CaTiSiO_5$: an infrared spectroscopic, dielectric response and heat capacity study. Physics and Chemistry of Minerals, 22, 41–49.

Zhong, W., Vanderbilt, D., and Rabe, K.M. (1994) Phase transitions in $BaTiO_3$ from first principles. Physical Review Letters, 73, 1861–1864.

——— (1995) First-principles theory of ferroelectric phase transitions for perovskites: the case of $BaTiO_3$. Physical Review B52, 6301–6312.

Appendix Table: Examples of phase transitions in minerals. Here are tabulated examples of phase transitions in minerals that occur with either a change in temperature or pressure extracted from an electronic search of the Science Citation Index for the years 1981–1996. In some cases details such as the symmetry change may still be unknown or uncertain (marked with a "?"). The transformation behavior of some materials may be affected by sample impurities, sample treatment, or kinetic factors, which can account for some uncertainties. Neither this listing nor the cited references are comprehensive but are designed to give a range of examples. References are listed below.

Material	T_c or P_c	Change	Comments
Quartz, SiO_2	848 K	$P6_222$–$P3_121$	Two-stage displacive phase transition involving an intermediate incommensurate phase. [1]
Cristobalite, SiO_2	530 K 1.2 GPa	$Fd3m$–$P4_12_12$ $P4_12_12$–$P2_1$	First-order displacive phase transitions involving zone-boundary instabilities. [2]
Tridymite, SiO_2	748 K 623 K	$P6_3/mmc$–$P6_322$ $P6_322$–$C222_1$	A number of displacive phase transitions occur on cooling. The two given here involve zone-center instabilities. [3]
Leucite, $KAlSi_2O_6$	960 K	$Ia3d$–$I4_1/acd$ $I4_1/acd$–$I4_1/a$	Two-stage displacive phase transition, the first being a ferroelastic phase transition. Other materials with the leucite structure but different chemical composition can undergo other displacive and order-disorder phase transitions. [4]
Albite, $NaAlSi_3O_6$	1250 K	$C2/m$–$C\bar{1}$	Ferroelastic phase transition. An Al-Si ordering transition follows at lower temperatures, but because this does not involve a further symmetry change it does not lead to a distinct transition temperature. Substitution of K^+ for Na^+ suppresses the ferroelastic phase transition, although the ordering transition is only weakly dependent on temperature. [5]
Anorthite, $CaAl_2Si_2O_6$	560 K	$I\bar{1}$–$P\bar{1}$	Displacive phase transition involving a zone-boundary instability. Substitution of Sr^{2+} for Ca^{2+} allows a ferroelastic phase transition to an $I2/m$ phase. [6]
Kalsilite, $KAlSiO_4$			A preliminary study indicates the presence of one or more phase transitions, but details remain sketchy. [7]
Kaliophilite, $KAlSiO_4$	1000 K	$P6_322$–$P6_3$(?)	Apparently a zone-center transition, but details are sketchy. [8]
Calcite, $CaCO_3$	1260 K 1.5 GPa	$R\bar{3}c$–$R\bar{3}m$ $R\bar{3}c$–$P2_1/c$	Orientational order-disorder phase transition involving the carbonate molecular ions. The ordering involves doubling of the size of the unit cell. An additional phase transition occurs at 2.2 GPa. [9]
Soda niter, $NaNO_3$	560 K	$R\bar{3}c$–$R\bar{3}m$	Orientational order-disorder phase transition involving the nitrate molecular ions. The ordering involves doubling of the size of the unit cell. [10]
Åkermanite, $Ca_2MgSi_2O_7$, and related melilites	343 K	$P\bar{4}2_1m$–Inc.	Incommensurate displacive phase transition. A possible phase transition to another commensurate phase at low temperatures has not yet been identified. [11]
Cordierite, $Mg_2Al_4Si_5O_{18}$		$P6/mcc$–$Cccm$	Al-Si ordering transition [12]
Perovskite, $CaTiO_3$	1384 K 1520 K	$Cmcm$–$Pbnm$ $Pm3m$(?)–$Cmcm$	Displacive phase transition involving tilt of TiO_6 octahedra, with evidence of phase transitions to tetragonal and cubic phases at higher temperatures. [13]
Titanate, $CaTiSiO_5$	497 K	$C2/c$–$P2_1/a$	Zone-boundary displacive phase transition. [14]
Staurolite		$Ccmm$–$C2/m$	Al-vacancy ordering transition. [15]
Colemanite, $CaB_3O_4(OH)_3 \cdot H_2O$	270 K	$P2_1/a$–$P2_1$	Ferroelectric phase transition. [16]
Chlorapatite, $Ca_5(PO_4)_3Cl$	620 K	$P6_3/m$–$P2_1/a$	Ferroelastic phase transition. [17]
Cryolite, Na_3AlF_6	820 K	$Immm$–$P2_1/n$	[18]
Langbeinite, $K_2Cd_2(SO_4)_3$		$P2_13$–$P2_12_12_1$	Transition temperature depends on composition, with several possible substitutions of the Cd^{2+} cation. [19]
Natrite (Gregoryite), Na_2CO_3	760 K	$P6_3/mmc$–$C2/m$	Ferroelastic phase transition involving the softening of the C_{44} elastic constant. [20]
Ilvaite, $CaFe_2Si_2O_2(OH)$	346 K	$Pnam$–$P2_1/a$	Phase transition driven by ordering of electrons on the Fe sites. [21]
Sodalites			Sodalites of different composition can undergo displacive phase transitions, Al-Si ordering phase transitions, and phase transitions involving orientational ordering of molecular ions in the large cavity coupled to displacive distortions of the sodalite framework. [22]
Brucite, $Mg(OH)_2$	6–7 GPa		Possible phase transition involving ordering of H atom. [23]

APPENDIX—*Continued.*

Garnets			Several postulated cation-ordering phase transitions based on different observed ordered structures. [24]
Material	T_c or P_c	Change	Comments
Gillespite, $BaFeSi_4O_{10}$	1.8 GPa	$P4/ncc$–$P2_12_12$	First-order phase transition, mostly displacive in character but also involving some changes in coordination. [25]
Ferrosilite, $FeSiO_3$	1.4–1.8 GPa	$C2/c$–$P2_1/c$	Displacive phase transition. Similar transitions are found in other pyroxenes. [26]
Arcanite, K_2SO_4	860 K	$P6_3/mmc$–$Pmcn$	Orientational ordering of SO_4^{2-} anions. [27]
Sanmartinite, $ZnWO_4$–scheelite, $CuWO_4$		$P2/c$–$P\bar{1}$	Jahn-Teller phase transition as a function of composition. [28]
Chiolite, $Na_5Al_3F_{10}$	150 K	$P4/mnc$–$P2_1/n$	Displacive phase transition. [29]
Schultenite, $PbHAsO_4$	313 K	$P2/c$–Pc	Ordering of the hydrogen bond. [30]

References:

[1] Berge et al. (1986); Bethke et al. (1987); Castex and Madon (1995); Dolino (1990); Dolino et al. (1989, 1992); Dolino and Vallade (1994); Dorner et al. (1981); Grimm and Dorner (1975); Heaney (1994); Heaney and Veblen (1991); Salje et al. (1992); Shapiro et al. (1967); Spearing et al. (1992); Tautz et al. (1991); Tezuka et al. (1991); Vallade et al. (1992)
[2] Dolino and Vallade (1994); Dove et al. (1995); Hatch and Ghose (1991); Heaney (1994); Hua et al. (1988); Palmer et al. (1994); Palmer and Finger (1994); Phillips et al. (1993); Schmahl et al. (1992); Schmahl (1993); Spearing et al. (1992); Swainson and Dove (1993a,b, 1995); Welberry et al. (1989); Withers et al. (1989, 1994); Wright and Leadbetter (1975)
[3] Cellai et al. (1994, 1995); de Dombal and Carpenter (1993); Heaney (1994); Kihara (1978, 1995); Withers et al. (1994); Xiao et al. (1993, 1995a)
[4] Bell et al. (1993, 1994); Boysen (1990); Dove et al. (1993, 1995); Hatch et al. (1990b); Heaney and Veblen (1990); Ito et al. (1991); Lange et al. (1986); Liu (1987); Palmer et al. (1989, 1990; 1997); Palmer and Salje (1990)
[5] Harris et al. (1989); Salje (1986); Xiao et al. (1995b)
[6] Daniel et al. (1995); Ghose et al. (1988, 1993); Hackwell and Angel (1995); Hatch and Ghose (1989a); McGuinn and Redfern (1994a, b); Phillips et al. (1992); Phillips and Kirkpatrick (1995); Redfern and Salje (1987, 1992); Redfern et al. (1988); Redfern (1992); Salje (1987); Tagai et al. (1988); Tribaudino et al. (1993); Van Tendeloo et al. (1989)
[7] Capobianco and Carpenter (1989)
[8] Cellai et al. (1992)
[9] Dove and Powell (1989); Dove et al. (1992b, c, 1997); Fiquet et al. (1994); Hagen et al. (1992); Liu and Mernagh (1990); Markgraf and Reeder (1985); Merrill and Bassett (1975); Redfern et al. (1989b)
[10] Harris et al. (1990); Lefebvre et al. (1984); Reeder et al. (1988)
[11] Brown et al. (1994); Hemingway et al. (1986); Li et al. (1990); Merwin et al. (1989); Rothlisberger et al. (1990); Seifert and Rothlisberger (1993); Webb et al. (1992)
[12] Gibbs (1966); Güttler et al. (1989b); Meagher and Gibbs (1977); Poon et al. (1990); Putnis et al. (1987); Redfern et al. (1989a); Thayaparam et al. (1996)
[13] Guyot et al. (1993); Wang and Liebermann (1993); Vogt and Schmahl (1993); Redfern (1996)
[14] Bismayer et al. (1992); Ghose et al. (1991); Salje et al. (1993); Van Heurck et al. (1991); Zhang et al. (1995)
[15] Hawthorne et al. (1993)
[16] Gallup and Coleman (1990)
[17] Bauer and Klee (1993)
[18] Separing et al. (1994); Yang et al. (1993)
[19] Boeriogoates et al. (1990); Devarajan and Salje (1986); Hatch et al. (1990a); Percival et al. (1989); Percival (1990); Speer and Salje (1986)
[20] Harris et al. (1993, 1995, 1996); Harris and Dove (1995); Swainson et al. (1995)
[21] Ghazibayat et al. (1992); Ghose et al. (1989); Güttler et al. (1989a); Kan et al. (1988)
[22] Depmeier (1988, 1992); Depmeier and Bührer (1991)
[23] Catti et al. (1995); Duffy et al. (1995)
[24] Hatch and Griffen (1989); Hatch and Ghose (1989a)
[25] Hazen and Finger (1983); Redfern et al. (1993, 1997)
[26] Hugh-Jones et al. (1994); Shimobayashi and Kitamura (1991); Sueno et al. (1985)
[27] Miyake et al. (1981); Miyake and Iwai (1981)
[28] Redfern (1993); Redfern et al. (1995); Schofield and Redfern (1992, 1993), Schofield et al. (1994)
[29] Spearing et al. (1994)
[30] Wilson (1994)